



Unveiling ancient diversity of long-tailed wasps (Hymenoptera: Megalyridae): new taxa from Cretaceous Kachin and Taimyr ambers and their phylogenetic affinities

Manuel Brazidec^{1,2,3}, Lars Vilhelmsen⁴, Brendon E. Boudinot^{5,6,7}, Adrian Richter^{5,8}, Jörg U. Hammel⁹, Evgeny E. Perkovsky^{4,10}, Yong Fan¹¹, Zhen Wang^{4,12}, Qiong Wu^{4,12}, Bo Wang³, Vincent Perrichot¹

1 Univ Rennes, CNRS, Géosciences Rennes, UMR 6118, 35000, Rennes, France

2 Institut de Systématique, Évolution, Biodiversité (ISYEB), Muséum national d'Histoire naturelle, CNRS, Sorbonne Université, EPHE, Université des Antilles, CP50, 57 rue Cuvier, F-75005 Paris, France

3 State Key Laboratory of Palaeobiology and Stratigraphy, Nanjing Institute of Geology and Palaeontology, Chinese Academy of Sciences, 39 East Beijing Road, Nanjing 210008, China

4 Natural History Museum of Denmark, SCIENCE, University of Copenhagen, Universitetsparken 15, DK-2100, Denmark

5 Institut für Zoologie und Evolutionsforschung, Friedrich-Schiller-Universität Jena, Vor dem Neutor 1, 07743 Jena, Germany

6 National Museum of Natural History, Smithsonian Institution, 10th & Constitution Ave. NW, Washington, DC, USA

7 Senckenberg Gesellschaft für Naturforschung und Naturmuseum, Frankfurt am Main, 60325 Germany

8 Biodiversity and Biocomplexity Unit, Okinawa Institute of Science and Technology Graduate University, Onna-son, Okinawa, Japan

9 Institute of Materials Physics, Helmholtz-Zentrum Hereon, Max-Planck-Str. 1, 21502 Geesthacht, Germany

10 I. I. Schmalhausen Institut of Zoology, National Academy of Sciences of Ukraine, B. Khmel'nitskogo 15, Kiev 01030, Ukraine

11 Fushun Amber Institute, Fushun 113005, China

12 College of Life Sciences, Capital Normal University, 105 Xisanhuanbeilu, Haidian District, Beijing 100048, China

<https://zoobank.org/43AC036E-93CC-4D79-939A-07DF54BE1A2D>

Corresponding author: Manuel Brazidec (manuel.brazidec@gmail.com)

Received 14 August 2023

Accepted 05 January 2024

Published 22 March 2024

Academic Editors Ricardo Pérez-de la Fuente,
Mónica M. Solórzano-Kraemer

Citation: Brazidec M, Vilhelmsen L, Boudinot BE, Richter A, Hammel JU, Perkovsky EE, Fan Y, Wang Z, Wu Q, Wang B, Perrichot V (2024) Unveiling ancient diversity of long-tailed wasps (Hymenoptera: Megalyridae): new taxa from Cretaceous Kachin and Taimyr ambers and their phylogenetic affinities. *Arthropod Systematics & Phylogeny* 82: 151–181. <https://doi.org/10.3897/asp.82.e111148>

Abstract

The Megalyridae are a small family of parasitoid wasps comprising eight extant genera (71 species) and six extinct genera (13 species). Here, we report eight new species from Late Cretaceous Kachin (Myanmar) and Taimyr (Russia) ambers; the family is recorded for the first time from the latter. †*Cretolyra nojebumensis* **gen. et sp. nov.**, †*Cretolyra shawi* **gen. et sp. nov.**, †*Genkyhag inebula* **gen. et sp. nov.**, †*Megacoxa chandrasahra* **gen. et sp. nov.**, †*Megacoxa janzeni* **gen. et sp. nov.**, and †*Megacoxa synchrotron* **gen. et sp. nov.**, are described from late Albian – early Cenomanian Kachin amber; †*Kamyristi exfrigore* **gen. et sp. nov.** and †*Kamyristi yantardakhensis* **gen. et sp. nov.** from Taimyr amber (Baikura, late Albian – early Cenomanian Ognevka Formation and Yantardakh, Santonian Kheta Formation, respectively). Phylogenetic analyses of the family are presented and the classification of the Megalyridae is revised accordingly. A new tribe, †*Megalavini* **trib. nov.**, is erected to accommodate †*Cretolyra* **gen. nov.**, †*Genkyhag* **gen. nov.**, †*Megacoxa* **gen. nov.** together with †*Megalava* Perrichot, 2009; †*Megalavini* **trib. nov.** is characterized by the vein M fully pigmented and veins Rs+M and M+Cu aligned, the crenulate mesometapectal sulcus, and the pronotal spiracle not posteriorly surrounded by cuticle. This spiracular condition was previously only observed in †*Megazar* Perrichot, 2009, thus the subfamily †*Megazarinae* Perrichot, 2009 **stat. nov.** is proposed for the clade (†*Megalavini* + †*Megazar*), as sister to the remaining Megalyridae. The latter is

defined as the Megalyrinae, with †*Kamyristi* **gen. nov.** being retrieved as sister to all other genera except *Rigel* Shaw, 1987 under parsimony analyses. To align phylogeny with classification, three new tribes are erected (†Kamyristini **trib. nov.**, †Megallicini **trib. nov.**, and †Valaaini **trib. nov.**) and the †Cretodinapsini is synonymized under Megalyrini. A grouping [*Rigel* + *Megalyridia*] is supported under Bayesian analyses, which is the only specific conflict with the parsimony analyses, suggesting some degree of caution with respect to the internal relationships of the Megalyrinae. Finally, a revised key to the Megalyridae genera is provided.

Keywords

Megalyroidea, Myanmar, Taimyr, Albian-Cenomanian, Santonian, phylogeny

1. Introduction

The Megalyridae are a small family of rarely collected parasitoid wasps that can currently be found principally, but not exclusively, in the southern hemisphere. The eight extant genera are widely distributed in the Neotropical, Afrotropical, Indomalayan, and Australasian regions, with limited occurrence in the eastern Palaearctic (Japan) (Vilhelmsen et al. 2010a; Mita and Konishi 2011). Shaw (1990a) stated that this predominantly pantropical distribution is the consequence of the occurrence of the family in the tropical forests of the supercontinent Pangea. The current distribution is probably relictual, being correlated with the general cooling of the climate in the last 40 Ma as well as transfer from Cretaceous and Eocene greenhouse climate to the current icehouse one, as exemplified by the occurrence of *Megalyra* Westwood in Baltic amber (†*Megalyra baltica* Poinar & Shaw, 2007), today found only in subtropical and tropical regions of Australasia (Shaw 1990b).

The type genus of the family, *Megalyra* Westwood, 1832, was originally described within the Ichneumonidae (Westwood 1832), but was later placed in its own family by Schletterer (1889). The Megalyridae may be separated from all hymenopteran families by a unique combination of characters, including the presence of a subantennal groove, the insertion of the antennae below the ventral margin of the eyes, the presence of 14 antennomeres, a distinctly arching mesoscutum that is divided by a well-developed median mesoscutal sulcus, the large triangular axillae on the mesoscutum, and a long ovipositor in female specimens (Shaw 1990b). However, the length of the ovipositor in most megalyrid genera is not exceptional compared to other parasitic wasps, except for some species of *Megalyra*, e.g., *M. lilliputiana* Turner, 1916 or *M. fasciipennis* Westwood, 1832 (Vilhelmsen 2003), and varies broadly across the family. Nevertheless, the names *Megalyra* and Megalyridae derive from this feature, as the ovipositor resembles a stringed instrument such as a lyre (Vilhelmsen et al. 2010a).

Earlier studies on the phylogeny of Hymenoptera retrieved Megalyridae in the Stephanoidea, within the larger Evaniomorpha clade (Rasnitsyn 1988; Ronquist et al. 1999). However, recent morphology-based works put the family in its own monotypic superfamily Megalyroidea (Dowton and Austin 2001; Vilhelmsen et al. 2010b). Dif-

ferent sister group relationships were suggested either with Stephanoidea (Rasnitsyn 2002), Trigonalioidea (Dowton et al. 1997; Castro and Dowton 2006), or Ceraphronoidea (Gibson 1985; Sharkey 2007; Vilhelmsen et al. 2010b; Sharkey et al. 2012). The Megalyridae have only recently been included in phylogenomic analyses (Blaimer et al. 2023); but their results, alongside mitochondrial analyses, congruently supported Trigonalioidea as sister to Megalyroidea (e.g., Klopstein et al. 2013; Mao et al. 2014; Tang et al. 2019). The phylogenetic placement of Megalyridae, Stephanoidea, and ‘Evaniomorpha’ is of high priority to resolve from the perspective of the fossil record and morphological evolution of the Apocrita (see, e.g., Rasnitsyn and Zhang 2010; Li et al. 2015).

The biology of Megalyridae is poorly known except for a few species of *Megalyra*, the most frequently collected genus. They are considered to be ectoparasitoids of beetle larvae belonging to the Bostrichidae, Cerambycidae, and Buprestidae, which live inside wood (Shaw 1990a). However, pupae of *M. troglodytes* Naumann, 1987 have been found in mud-nesting larvae of Crabronidae (Naumann 1987). This comes in addition to a single observation of Noble (1933, 1936) of an unidentified *Megalyra* emerging from the woody gall of Eurytomidae (*Bruchophagus fellis* (Girault, 1928)). However, Noble could not confirm if the gall was actually occupied by this wasp or by a beetle larva (Noble 1936). Apparently, female megalyrids prefer to explore pre-existing cracks or frass to oviposit (Mesaglio and Shaw 2022), although Rodd (1951) described an instance of active drilling.

The low number of extant species reflects the lack of knowledge and the legitimately poor diversity of the Megalyridae (Appendix S1). Most genera contain only few species. In East Asia, *Carminator* Shaw, 1988 is represented by nine species (Mita and Konishi 2011; Chen et al. 2021), with *C. japonicus* Mita & Konishi, 2011 being the northernmost record of a megalyrid; *Etchellsia* Cameron, 1909 from Asia by seven (Chen et al. 2021); in South America, *Cryptalyra* Shaw, 1987 by six (Kawada et al. 2014). *Neodinapsis* Shaw, 1987, *Rigel* Shaw, 1987 and the South African *Megalyridia* Hedqvist, 1959 are monospecific (Perrichot 2009; van Noort and Shaw 2009). The two most speciose genera are *Megalyra*, which is represented by 27 extant species (Vilhelmsen et

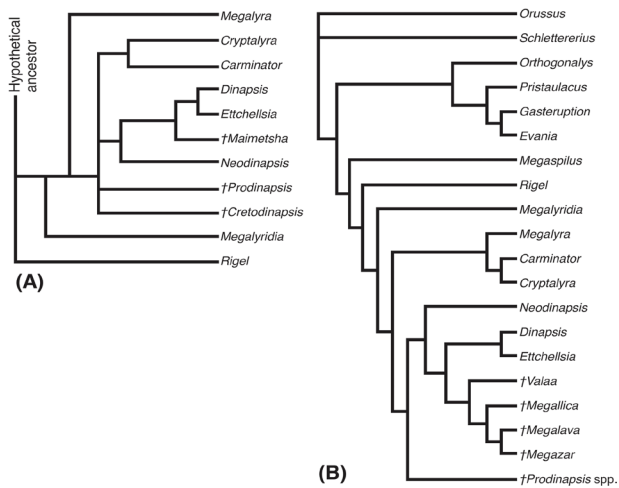


Figure 1. Previously published cladograms for the Megalyrinae: **A** from Shaw (1990a: fig. 5); **B** from Vilhelmsen et al. (2010a: fig. 8).

al. 2010a), and *Dinapsis* Waterston, 1922, with 19 species (van Noort et al. 2022). Given the presence of many undescribed *Dinapsis* species in Madagascar (van Noort et al. 2022), it is likely that this genus will eventually surpass *Megalyra* in terms of described diversity.

Shaw (1990a) and Vilhelmsen et al. (2010a) carried out taxonomic and phylogenetic revisions of the Megalyrinae (Fig. 1), the latest resulting in the synonymization of †*Ukrainosa* Perrichot, 2009 and †*Rubes* Perrichot, 2009 under †*Prodinapsis* Brues, 1923. Since this revision, the only addition to the knowledge of the fossil diversity is the description of the male †*Megalava truncata* Perrichot, 2009 (Pérez-de la Fuente et al. 2012). This is surprising as representatives of the family are known from Canadian amber (M. Engel pers. comm. in Perrichot 2009), Raritan amber (Grimaldi et al. 2000), and Kachin amber (Grimaldi et al. 2002; Grimaldi and Engel 2005; Xia et al. 2015; Zhang et al. 2018; Rasnitsyn and Öhm-Kühnle 2021).

In this contribution, we describe eight new species in four new genera of Megalyrinae, based on 12 specimens from Kachin and Taimyr deposits. The systematic positions of these new taxa are explored using maximum parsimony and Bayesian analyses. Note that we follow the definition of Megalyrinae of Perrichot (2009) and Vilhelmsen et al. (2010a), since different taxa have been assigned to Megalyrinae but are not still consensually accepted as such (e.g., †*Cleistogastrinae*; Rasnitsyn 1975).

2. Material and methods

2.1. Amber specimens

Kachin amber. Ten of the fossil specimens examined for the present study are inclusions in amber pieces from the deposits of Noije Bum in the Hukawng Valley (26°29'N, 96°35'E), Kachin State, northern Myanmar (see detailed

map in Grimaldi and Ross 2017: fig. 2). Radiometric data and taphonomic analysis of Pholadidae (Mollusca: Bivalvia) established an early Cenomanian age (98.79 ± 0.62 Ma) for Kachin amber, based on zircons from volcanic clasts found within the amber-bearing sediments (Shi et al. 2012; Smith and Ross 2018). Some ammonites (Mollusca: Cephalopoda) found in the amber-bearing bed and as amber inclusions corroborate a late Albian – early Cenomanian age (Cruikshank and Ko 2003; Yu et al. 2019). Specimens IGR.BU-067 to 069 were first accessed from the private collection of Jens-Wilhelm Janzen (Sevetal, Germany) and were subsequently purchased for permanent deposition in the amber collection of the Geology Department and Museum of the University of Rennes, France (**IGR**). Specimen CASENT0753237 was first accessed from the private collection of Sieghard Ellenberger (Kassel, Germany) and subsequently purchased for permanent deposition in the amber collection of the Phyletisches Museum Jena (**PMJ**). Specimen CNU-HYM-MA2016207 was accessed by Z.W. and Q.W., and is housed in the Key Lab of Insect Evolution and Environmental Changes, College of Life Sciences, Capital Normal University, Beijing, China (CNU). Specimens NIGP203545 to NIGP203547 were accessed by B.W., and are housed in the Nanjing Institute of Geology and Palaeontology (**NIGP**), Chinese Academy of Sciences, Nanjing, China. Finally, the amber piece FAI-BI 11324, with three specimens (11324a to 11324c), is housed in the Fushun Amber Institute (**FAI**), Fushun, Liaoning Province, China.

Taimyr amber. Two specimens in two different pieces from the Paleontological Institute of the Russian Academy of Sciences (**PIN**) collection are described. PIN 3730/411 was found on the southern shore of the Lake Taimyr (Baikura locality). The age remains controversial due to a lack of paleofloristic data: Rasnitsyn et al. (2016) consider it to be either Turonian, according to the abundance of ants and chalcidoids, or perhaps upper Cenomanian, as the insect assemblage is similar to that of Agapa locality. Later contributions suggest that the Baikura assemblage is nearly the same age as Kachin amber (late Albian – early Cenomanian: Perkovsky and Wegierek 2017; Gumovsky et al. 2018; Perkovsky and Vasilenko 2019). PIN 3311/2718 was collected in the Yantardakh Lagerstätte (right bank of the Maymecha River, 3 km upstream from its confluence with the Kheta River (a left tributary of the Khatanga River), Yantardakh Hill) in the Kheta Formation, dated Santonian (Rasnitsyn et al. 2016).

2.2. Amber preparation and morphological examination

The amber pieces were polished to facilitate the observation of the inclusions, using thin silicon carbide papers on a grinder polisher (Buehler MetaServ 3000). The examination and photographs were conducted with a Leica DMC4500 camera attached to a Leica M205C

stereomicroscope. All images are digitally stacked photomicrographic composites of several focal planes, which were obtained using Helicon Focus 6.7. Adobe Illustrator CC2019 and Photoshop CC2019 software were used to compose the figures and ImageJ 1.53 for measurements. The description of the characters follows the terminology of Perrichot (2009) and Vilhelmsen et al. (2010a) and the surface sculpturing follows Huber and Sharkey (1993).

Abbreviations used in figures and text: **AG** = inner axillar groove; **BL** = body length; **Cx** = coxa; **F1, 2, 3 ...** = flagellomere 1, 2, 3 ...; **MMS** = median mesoscutal sulcus; **MeS** = mesometapectal sulcus; **OC** = occipital carina; **OL** = ovipositor length; **OvS** = ovipositor sheaths; **pa** = parameres; **pe** = pedicel; **PpL** = parapsidal line; **sc** = scape; **sp** = anterior thoracic spiracle.

2.3. Synchrotron Micro-Computed Tomography and Rendering

The amber specimen CASENT0753237 was scanned using synchrotron-radiation based micro-computed tomography (SR- μ -CT), which was performed at the Imaging Beamline P05 (IBL) (Haibel et al. 2010; Greving et al. 2014; Wilde et al. 2016) operated by the Helmholtz-Zentrum Hereon at the storage ring PETRA III (Deutsches Elektronen Synchrotron—DESY, Hamburg, Germany). For imaging, a photon energy of 18 keV and a sample to detector distance of 30 cm was used. Projections were recorded using a 50 MP CMOS camera system with an effective pixel size of 0.46 μ m. For each tomographic scan 4001 projections were recorded at equal intervals between 0 and π , with an exposure time of 350 ms. Tomographic reconstruction was done by applying a transport of intensity phase retrieval and using the filtered back projection algorithm (FBP) implemented in a custom reconstruction pipeline (Moosmann et al. 2014) using MATLAB (MathWorks) and the Astra Toolbox (Palenstijn et al. 2011; van Aarle et al. 2015, 2016). For further processing, raw projections were binned two times resulting in an effective pixel size of the reconstructed volume of 0.913 μ m. The resultant 32-bit .tif image sequence was then converted to 8bit files and down sampled twofold with Fiji (Schindelin et al. 2012), resulting in an effective pixel (voxel) size of 1.826 μ m.

We segmented the body using Amira 6.1 (Visage Imaging GmbH, Berlin, Germany). For the head, structures of interest were manually marked on every 10th slice in the region of the mandible and every 40th slice for the remaining head capsule, then Biomedisa (Lösel et al. 2020) was used to semiautomatically completed the segmentation. For the postcephalic body, the structures of interest were segmented using a variety of thresholding techniques followed by fastidious manual segmentation to clean up the label set and to capture regions that could not be labeled efficiently using thresholds. After manual corrections, segmented labels were exported as .TIF image stacks with the plugin script “multiExport” (Engelkes et al. 2018) in Amira 6.1. VG-Studio Max 3.4 (Volume

Graphics GmbH, Heidelberg, Germany) and the Volume Render function of Amira were used for volume rendering of the labeled structures.

2.4. Phylogenetic analyses

The phylogenetic part of this study is primarily based on Vilhelmsen et al. (2010a) (see the character list in Appendix S1). The aim of the analyses conducted here is to evaluate the position of the newly described taxa and how their inclusion affects the overall Megalyridae phylogeny (Table 1).

Among the outgroup terminals, we included *Orthogonalys* Schulz, 1905 (Trigonalynoidea: Trigonalynoidea), *Pristaulacus* Kieffer, 1900 (Evanioidea: Aulacidae) and *Schlettererius* Ashmead, 1900 (Stephanoidea: Stephanoidea) to test the monophyly of Megalyridae. In order to code the new characters for the outgroup taxa, several specimens of *Orthogonalys pulchella* (Cresson, 1880), *Pristaulacus strangaliae* Rohwer, 1917 and *Schlettererius cinctipes* (Cresson, 1880) from the collection of the Natural History Museum of Denmark were examined. The relationships of the †Maimetshidae with the Megalyridae were explored in Vilhelmsen et al. (2010a); in most analyses †Maimetshidae fell outside Megalyridae. The discoveries of new taxa (Perrichot et al. 2004; Rasnitsyn and Brothers 2009; Engel 2016) allowed the definition of †*Maimetsha* Rasnitsyn, 1975 and other related fossils as the distinct family †Maimetshidae, hence we decided to exclude them from the analyses.

To code extant and extinct Megalyridae in the matrix, most of the original material could not be accessed. Therefore, the characters were scored from the relevant literature, specimens housed in the amber collection of the Geological Department and Museum of the University of Rennes, France, or SEM images from Vilhelmsen et al. (2010a). This includes the description of the male of †*M. truncata* by Pérez-de la Fuente et al. (2012). Finally, as the monophyly of †*Prodinapsis* has been previously demonstrated (Vilhelmsen et al. 2010a) and to avoid the calculation of all the possible topologies between the seven species of this genus, we treated them in three different ways in the analyses: 1) group all the species in one terminal, 2) group only the three species with the fewest missing entries (i.e., †*P. succinalis* Brues, 1923 the type species of †*Prodinapsis*, plus †*P. prolata* (Perrichot & Perkovsky, 2009) and †*P. bruesi* (Perrichot, 2009)) in one terminal, and 3) include the three species with the fewest missing entries as separate terminals. These three solutions produced similar results in terms of the position of †*Prodinapsis*.

Cladistic analyses were carried out using TNT 1.5 (Goloboff and Catalano 2016). The following characters were treated as additive: 8, 18, 38, 39, 47. Space for 99,999 trees was reserved in memory and traditional searches were run with implied-weights, with collapsing rules set to minimum length = 0 and with the concavity k set to 3, 5 or 10. One thousand replications with 1000 trees saved per replication were run. Trees were rooted on

Table 1. Morphological data matrix for phylogenetic analyses.

Taxon	Characters					Missing/ inappli- cable entries
	1–10	11–20	21–30	31–40	41–49	
<i>Schlettererius</i>	00-0001100	0011000001	0110010001	0000001110	000001020	
<i>Orthogonalys</i>	10-0001110	0001100000	0111101100	0000110010	000001012	0/1
<i>Pristaulacus</i>	10-1000100	0001011000	0111101102	0000010010	000011021	
<i>Carminator</i>	01[01]1110200	1021[01]11210	001[01]?10001	01000012-2	--1100302	1/3
<i>Cryptalyra</i>	01111101?0	101001?211	1011?100[01]2	?110??12-2	001100312	6/1
<i>Dinapsis</i>	011101010[01]	[01]110011211	101010[01]01[012]	0101000020	001110221	
<i>Ettchellsia</i>	01110[01]0100	[01]110011211	1010100110	0101000020	001010222	
<i>Megalyra</i>	01110[01]010[01]	[01]01101121[01]	1000111102	0110000[012]02	00[01]0100[12]0	
<i>Megalyridia</i>	0111000100	0000011211	1010101001	00000002-2	001110111	0/1
<i>Neodinapsis</i>	011?0?01?0	0110?11211	1010?01101	0000000020	001100112	5/0
<i>Rigel</i>	0101000100	1000011201	1010101001	0000000111	001101111	
† <i>Cretodinapsis</i>	?????????1	?0?011??1	?000??????	0?????0212	010001212	26/0
† <i>Cretolyra nojebumensis</i>	0101000100	0010011111	10102110?0	1010??0010	110000?2?	5/0
† <i>Cretolyra shawi</i>	0101000100	0010011101	10112110?0	1010??0010	110000?22	4/0
† <i>Genkyhag innebula</i>	0101010100	00100111?1	?01011?0?0	1000??0010	110000?22	8/0
† <i>Kamyristi exfrigore</i>	01?100?100	0010111211	00011000?1	0110??0021	001101?1?	7/0
† <i>Kamyristi yantardakhensis</i>	0101000100	0010111201	00001?????	0110??0021	001101?1?	9/0
† <i>Megacoxa chandrasahsa</i>	0101010100	0010011101	10102010?0	1000??0010	110000?22	5/0
† <i>Megacoxa janzeni</i>	0101010100	0010011101	10112010?0	1000??0010	110000?22	4/0
† <i>Megacoxa synchrotron</i>	0101010??0	0010011101	10112010?0	1000??0010	110000?2?	8/0
† <i>Megalava</i>	01?100?1?1	0010111??1	0010?110??	[01]00?000010	110000?2?	11/0
† <i>Megallica</i>	0101110101	0011011?01	00011?10?0	0000000021	0-1100?1?	5/1
† <i>Megazar</i>	0101000200	0011111111	0010110000	1000000020	010000321	
† <i>Prodinapsis bruesi</i>	0101110101	1110011211	1001111002	00000002-2	0-1000112	0/2
† <i>Prodinapsis prolata</i>	0111001101	1010011211	100110?0?0	0000000222	0-1000111	2/1
† <i>Prodinapsis succinalis</i>	0111[01]01101	1110011211	1001101002	0000000220	0-1000112	0/1
† <i>Prodinapsis</i>	01[01]1[01][01][01]101	1[01]10011211	10011[01]100[02]	000000022[02]	0-100011[12]	0/1
† <i>Valaa</i>	0101010100	00?0011211	100110?0?0	0000000020	00110022?	4/0

Schlettererius. Considering the numerous missing entries of †*Cretodinapsis* Rasnitsyn, 1977 (53%), we ran additional analyses under the same parameters but without this taxon, to see how its absence affected the topologies.

Morphology-only Bayesian analyses were carried out using MrBayes 3.2.6 (Ronquist et al. 2012). The morphological data were analyzed in a single partition and were treated as unordered, except characters 8, 18, 38, 39 and 47, similarly to the parsimony analyses. We compared the Mk_v and Mk_v+G models (Lewis 2001; Yang 1993) using stepping stone integration (Xie et al. 2011), with +G accounting for among-character rate variation. The stepping stone analyses were performed for 2.5 million generations over 50 steps with an alpha of 0.4 and sampling every 100th generation across two runs with four chains each. For topology searches, MCMC was performed for at least 5 million generations sampling every 1,000th generation across two runs with four chains each, with a temperature of 0.01 and a diagnostic burnin fraction of 0.1. These analyses were run until the average deviation of split frequencies (ASDSF) was well below 0.01 for several thousand generations and when the potential scale

reduction factor (PSRF) for each factor approximated 1.00. At the end of each run, the estimated sample sizes (ESS) for each variable were checked with Tracer 1.7.1 (Rambaut et al. 2018); if the ESSs were below 300, we ran the topology searches for additional generations. We also used Tracer to determine the burn-in value for tree and parameter summary. The resulting trees were summarized as ‘half compatible’, i.e., with a 0.5 Bayesian posterior probability cutoff (= 50% majority tree rule) using the ‘sumt contype’ command in the MrBayes input. Finally, because of one conflicting topological result (*Rigel* + *Megalyridia*), we ran an ancestral state estimation analysis by constraining Megalyridae, †Megazarinae, Megalyrinae, *Rigel* + *Megalyridia*, and *Megalyra* + †*Cretodinapsis* + †*Prodinapsis* + *Carminator* + *Cryptalyra*. We turned on the ancestral state monitor at these nodes and ran the analysis as for the topology searches above under the Mk_v model. We then copy-pasted the parameter statistics (“pstat”) results into an Excel spreadsheet and evaluated transitions and their support following the method of Richter et al. (2022).

3. Systematic Palaeontology

Order: Hymenoptera Linnaeus, 1758

Superfamily: Megalyroidea Schletterer, 1889

Family: Megalyridae Schletterer, 1889

Dinapsidae Waterston, 1922

Type genus. *Megalyra* Westwood, 1832.

Emended diagnosis. Head usually hypognathous, prognathous in *Carminator*; antenna filiform, inserted below level of ventral margin of eye, with 12 flagellomeres, scape usually short and globular, elongate and flattened in *Carminator*; subantennal groove present, with or without dorsal carina; eye large, with posterior orbit smooth or delimited by a groove and/or postocular carina; mandible with three to five teeth. Pronotum reduced medially, barely visible dorsally; mesoscutum large, arched in lateral view, with parapsidal lines sometimes present; median mesoscutal sulcus present; notaulus absent; axilla large, triangular; anterior thoracic spiracle visible, usually completely surrounded by pronotal cuticle, exposed posteriorly in some Cretaceous fossils. Fore wing with at least veins Sc+R, A, Rs+M and r-rs pigmented; other veins C, M+Cu, Cu, R1, Rs and M in various configuration from pigmented to spectral. Hind wing without enclosed cells, with Rs usually not extended beyond middle of wing. Metacoxa large, metafemur swollen. First metasomal segment inserted low on propodeum, very close to metacoxal foramina; ovipositor external, at least half as long as metasoma.

3.1. Subfamily †Megazarinae Perrichot, 2009 stat. nov.

Type genus. †*Megazar* Perrichot, 2009.

Diagnosis. Head hypognathous, globular; compound eye oval, not covering head length, without postocular carina; flagellomeres cylindrical, longer than wide; subantennal groove without dorsal carina; mandibles symmetrical, with three or four teeth. Posterolateral margin of pronotum with notch accommodating anterior thoracic spiracle, not surrounding spiracle posteriorly; mesoscutum large, around half length of mesosoma, parapsidal lines present; median mesoscutal sulcus and axillar grooves present, deeply crenulate or smooth. Metasoma elongate. Fore wing hyaline; C, Sc+R, M+Cu, A, Rs+M, cu-a, Cu, Rs and R1 pigmented; costal, radial, first cubital, submarginal, and marginal cells closed by tubular veins. Hind leg stout, metafemur and metatibia swollen; at least either inner margin of metatrochanter, metacoxa, metatibia, or metabasitarsus bearing row of comb-like, thick setae along ventral surface.

Genera included. †*Cretolyra* gen. nov., †*Genkyhag* gen. nov., †*Megacoxa* gen. nov., †*Megalava* Perrichot, 2009 [†*Megalavini* trib. nov.]; †*Megazar* Perrichot, 2009 [†*Megazarini* Perrichot, 2009].

Stratigraphic extension. Albian to Cenomanian.

Comments. The tribe Megazarini Perrichot, 2009 is here elevated to subfamily level, as †*Megazarinae* stat. nov. based on the results of our phylogenetic analyses. The monophyly of the subfamily is supported by three synapomorphies under parsimony: (1) metatibia and/or metatarsus with comb-like setae along ventral surface (31:1; Fig. 3A); (2) fore wing Rs+M located posteriorly, with the submarginal cell being at least twice the size of the medial cell (42:1; Fig. 3C); and (3) fore wing pterostigma absent or reduced (46:0; Fig. 3C). Within the subfamily, a new tribe is created to accommodate three of the newly described genera and †*Megalava*.

3.1.1. Tribe †Megalavini trib. nov.

Type genus. †*Megalava* Perrichot, 2009.

Diagnosis. Mandible with three teeth, decreasing in size from apex to base; occipital carina crenulate. Pronotum not visible dorsally; mesometapectal sulcus (sensu Vilhelmsen et al. 2010b) crenulate. Fore wing venation most complete within Megalyridae; pterostigma reduced; C, M+Cu, Sc+R, A and M almost fully pigmented; R1 extending beyond marginal cell; marginal cell closed by Rs in straight line; Rs present between r-rs and Rs+M, closing first submarginal cell; M+Cu aligned with Rs+M; medial cell rectangular or trapezoidal, located under Rs+M and closed by 1m-cu and basal segments of Cu and Cu1. Metasoma elongate, with long to very long ovipositor (OL/BL ~ 0.40).

Genera and species included. †*Megalava truncata* Perrichot, 2009, †*Cretolyra noijebumensis* gen. et sp. nov., †*Cretolyra shawi* gen. et sp. nov., †*Genkyhag innebula* gen. et sp. nov., †*Megacoxa chandrahra* gen. et sp. nov., †*Megacoxa janzeni* gen. et sp. nov., †*Megacoxa synchrotron* gen. et sp. nov.

Comments. The †*Megalavini* trib. nov. retain a plesiomorphic fore wing venation (i.e., the most complete wing venation among megalyrids sensu stricto) as a key character with C, Sc+R, M+Cu, A, Rs+M, Cu, R1, Rs and M almost fully pigmented (Figs 2A–F). The main synapomorphy for this clade is the form of the medial cell, which is rectangular due to alignment of Rs+M with M+Cu (Figs 2A–F). Comprising exclusively Cretaceous taxa, †*Megalavini* trib. nov. also display an anterior thoracic spiracle that is not fully surrounded by pronotal cuticle (Fig. 3D), which we consider to be the second diagnostic feature (despite being plesiomorphic) for the tribe. When described, the monospecific genus †*Megalava* was stated to belong to the tribe †*Megazarini* with †*Megazar*, and this has been confirmed in Vilhelmsen et al. (2010a).

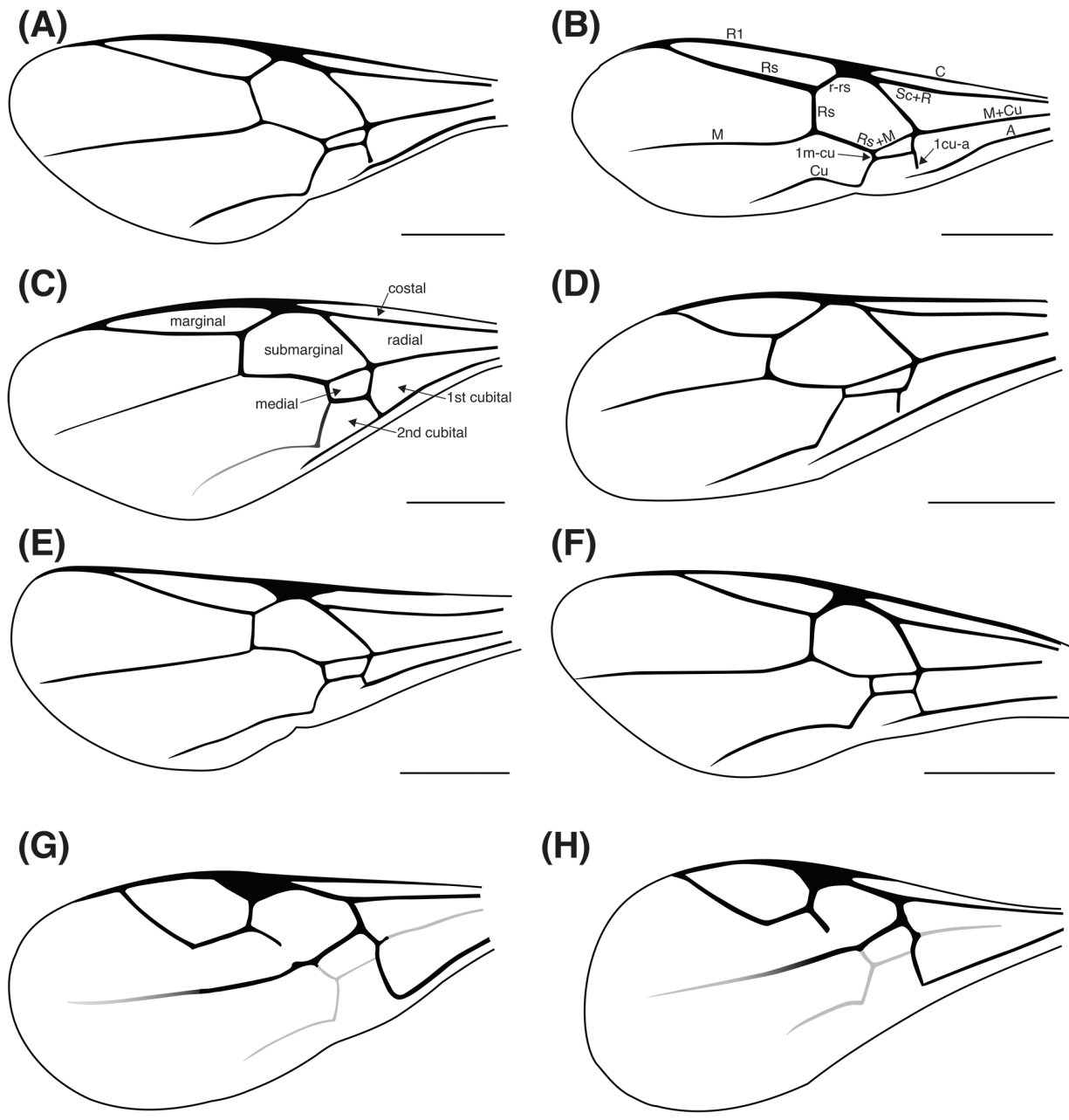


Figure 2. Drawings of fore wing venation for the taxa described in the present paper. **A** †*Cretolyra noihebumensis* gen. et sp. nov.; **B** †*Cretolyra shawi* gen. et sp. nov.; **C** †*Genkyhag innebula* gen. et sp. nov.; **D** †*Megacoxa chandraharsa* gen. et sp. nov.; **E** †*Megacoxa janzeni* gen. et sp. nov.; **F** †*Megacoxa synchronotron* gen. et sp. nov.; **G** †*Kamyrusti exfrigore* gen. et sp. nov.; **H** †*Kamyrusti yantardakhensis* gen. et sp. nov. Scale bars: 0.5 mm (A–H).

However, based on the description of a new complete specimen (Pérez-de la Fuente et al. 2012: fig. 2B), we propose to transfer †*Megalava* to the new tribe, due its more complete wing venation, the rectangular medial cell, the crenulate mesometapectal sulcus and the mandible configuration (three teeth while †*Megazar* has four).

3.1.1.1. Genus †*Cretolyra* gen. nov.

<https://zoobank.org/0190F601-F697-428D-BA66-B522AF1406E4>

Type species. †*Cretolyra noihebumensis* sp. nov.

Etymology. Combination of *Creto-* referring to the Cretaceous age of the Burmese amber deposit and the suffix *-lyra* often used in megalyrid genus names. Gender feminine.

Diagnosis. Compound eye oval, higher than long; frons longitudinally divided by sulcus anterior to median ocellus; flagellomere 1 shorter than individual length of flagellomeres 2–5; occipital carina crenulate. Fore wing with M+Cu, Sc+R, A, M and Cu fully pigmented; cu-a almost branching with A, absent for short distance; medial cell rectangular; marginal cell narrow, closed in straight line (Figs 2A, B, 3C and 4A). Median mesoscutal sulcus smooth; parapsidal lines pres-

ent, diverging anteriorly (Figs 3B and 4A). Metacoxa long; metafemur and metatibia swollen; two mesotibial and one metatibial spurs; row of comb-like setae along ventral surface of metatibia and metabasitarsus. Metasoma elongate and narrowed at apex, longer than mesosoma.

3.1.1.1.1. †*Cretolyra noijebumensis* sp. nov.

<https://zoobank.org/5C43B26B-D68E-45EC-9E3F-47C229B98AB7>

Figures 2A, 3

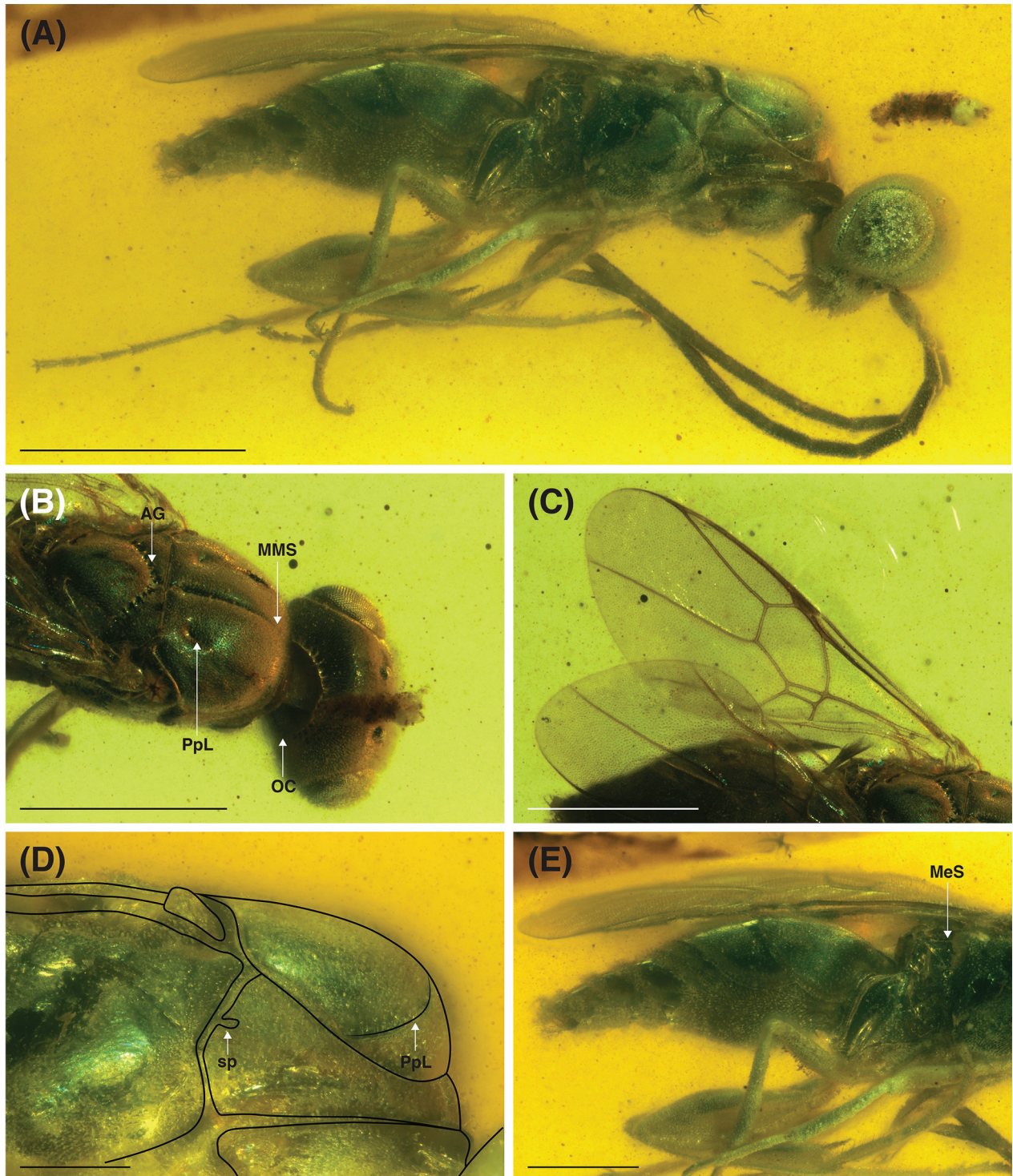


Figure 3. †*Cretolyra noijebumensis* gen. et sp. nov., holotype male IGR.BU-067, mid-Cretaceous, Kachin amber. **A** habitus in lateral view; **B** head and mesosoma in dorsal view; **C** fore wing; **D** anterior part of mesosoma in lateral view with structures outlined; **E** metasoma and posterior part of the mesosoma in lateral view. Scale bars: 0.5 mm (**A**, **B**, **C**, **E**); 0.25 mm (**D**). Abbreviations: AG = inner axillar groove; MeS = mesometapectal sulcus; MMS = median mesoscutal sulcus; OC = occipital carina; PpL = parapsidal line; sp = anterior thoracic spiracle.

Etymology. The specific epithet is an adjective referring to the type locality where the amber pieces were collected.

Material studied. *Holotype* male IGR.BU-067; housed in the amber collection of the Geology Department and Museum of the University of Rennes, France (IGR).

Type locality. Noiye Bum Hill, Hukawng Valley, Kachin State, Myanmar.

Age. Upper Albian to lower Cenomanian, mid-Cretaceous.

Diagnosis. Antennae inserted on edge of clypeus (Fig. 3A; vs. inserted above clypeal margin in *Cretolyra shawi* **gen. et sp. nov.**); axillae contiguous medially and axillar grooves crenulated (Fig. 3B; vs axillae separated medially and axillar grooves smooth in *Cretolyra shawi* **gen. et sp. nov.**).

Description. Body length 3.33 mm; body very pubescent, especially on metasoma where setae conceal margins of tergites; the setae have agglomerated small bubbles that make observation difficult. — **Head** globular, higher than long (length 0.55 mm; height 0.75 mm); frons convex, smooth, divided by thin median sulcus; compound eye oval, higher than long; vertex convex, with smooth ocellar triangle; clypeus well-developed; torulus inserted closer to clypeus than to eye; shallow but distinct subantennal groove adjoining ventral margin of eye; antenna half as long as body, almost reaching metasoma; scape twice as long as wide (length 0.16 mm); pedicel shorter than scape (length 0.11 mm); flagellomeres cylindrical, elongate, longer than wide; flagellomere 1 shortest (length 0.15 mm); following flagellomeres longer (length ca. 0.21 mm); occipital carina crenulate. — **Mesosoma** almost half body length (length 1.29 mm; height 0.65 mm); mesoscutum convex, shagreened, divided by smooth median mesoscutal sulcus (mesoscutum length 0.58 mm; width ~0.60 mm); parapsidal lines present, diverging anteriorly; axillae contiguous medially, axillar groove crenulate; mesoscutellum diamond-shaped; pronotum smooth, not visible dorsally, with posteromedial part moderately high as viewed laterally; anterior thoracic spiracle not fully surrounded by pronotal cuticle; mesometapectal sulcus crenulate; propodeum shorter than mesoscutellum, with incomplete pairs of median and submedian carinae, two complete lateral longitudinal carinae, anterior region of propodeum with transversal row of foveae adjacent to concealed metanotum, posterior region of propodeum with three large foveae. — **Fore wing** hyaline and covered with microtrichiae, about two thirds of body length (length 2.50 mm); C, Sc+R, M+Cu, A, Rs fully pigmented; R1 extending beyond marginal cell; Rs closing marginal cell in straight line; M pigmented to apex; medial cell rectangular, narrow; Cu almost reaching posterior wing margin. — **Legs** covered with setae; two mesotibial and one metatibial spurs; metacoxa elongate; metafemur and metatibia swollen; metabasitarsus three times as long

as following metatarsomeres and with row of short comb-like setae along ventral surface. — **Metasoma** half body length (length 1.48 mm), elongate and narrowed at apex; seven smooth tergites with pubescent posterior margin; first tergite largest; second tergite one quarter of metasoma length; remaining tergites shorter.

3.1.1.1.2. †*Cretolyra shawi* sp. nov.

<https://zoobank.org/8750B145-2332-49F3-BBED-7DEDA2A928CF>

Figures 2B, 4

Etymology. The specific epithet is a patronym honoring Scott R. Shaw, for his contributions to the knowledge of Megalyridae.

Material studied. *Holotype* female NIGP203545; housed in the Nanjing Institute of Geology and Palaeontology (NIGP), Chinese Academy of Sciences, Nanjing, China.

Type locality. Noiye Bum Hill, Hukawng Valley, Kachin State, Myanmar.

Age. Upper Albian to lower Cenomanian, mid-Cretaceous.

Diagnosis. Pedicel bilobed, long and thick (Figs 4D–E; vs. calciform and elongate in *Cretolyra noiyebumensis* **gen. et sp. nov.**); axillae almost rounded and reduced on edges of mesoscutellum, not contiguous medially (vs. contiguous medially in *Cretolyra noiyebumensis* **gen. et sp. nov.**); axillar grooves smooth (Fig. 4A; vs. axillar grooves crenulated in *Cretolyra noiyebumensis* **gen. et sp. nov.**); medial cell nearly triangular, with 1m-cu very short (Fig. 2B; vs. medial cell rectangular, with 1m-cu distinct in *Cretolyra noiyebumensis* **gen. et sp. nov.**).

Description. Body length 2.82 mm. — **Head** globular, higher than long (length ca. 0.40 mm), covered with short setae; frons convex, smooth, divided by sulcus; compound eye oval, higher than long; vertex convex; clypeus smooth, apically rounded; mandibles symmetrical, with three teeth; toruli separated from each other by less than their own diameter; subantennal groove present; antenna about half body length; scape shorter than pedicel; pedicel thick, bilobed; flagellomeres cylindrical, longer than wide; flagellomere 1 shorter than flagellomeres 2–5 (length 0.15 mm vs. ca. 0.21 mm); flagellomeres 6–11 shorter (length ca. 0.10 mm); flagellomere 12 as long as flagellomere 1 (length 0.15 mm); occipital carina minutely crenulate. — **Mesosoma** one third of body length (length 0.98 mm); mesoscutum convex, divided by smooth median mesoscutal sulcus; parapsidal lines present; axillae small, almost rounded and not contiguous medially; axillar groove smooth; mesoscutellum smooth, convex, diamond-shaped; pronotum smooth, not visible

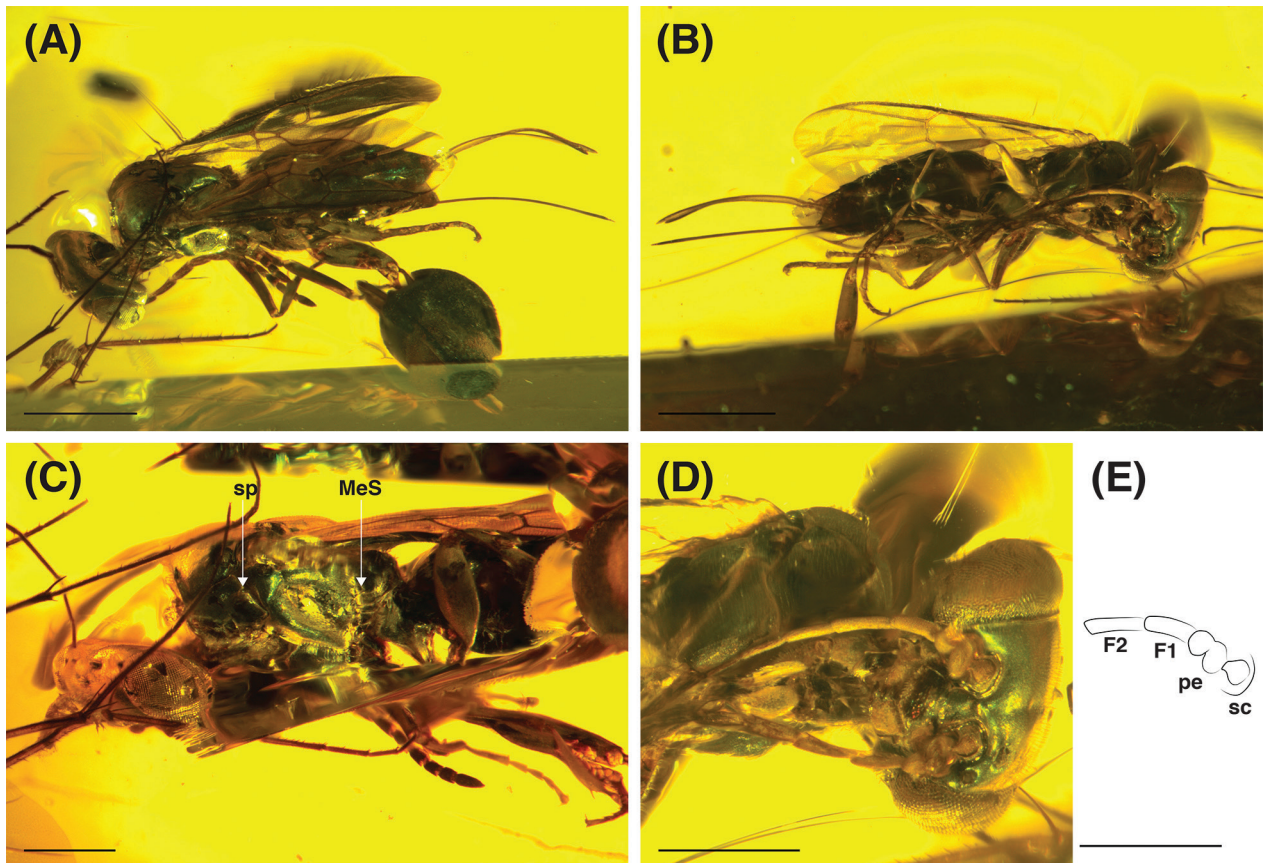


Figure 4. †*Cretolyra shawi* gen. et sp. nov., holotype female NIGP203545, mid-Cretaceous, Kachin amber. **A** habitus in dorsal view; **B** habitus in latero-ventral view; **C** head and mesosoma in lateral view; **D** head in frontal view; **E** line drawing of left scape, pedicel and flagellomeres 1 and 2. Scale bars: 1 mm (**A**, **B**); 0.5 mm (**C**, **D**, **E**). Abbreviations: F1 = flagellomere 1; F2 = flagellomere 2; MeS = mesometapectal sulcus; pe = pedicel; sc = scape; sp = anterior thoracic spiracle.

dorsally, with posteromedial part moderately high as viewed laterally; anterior thoracic spiracle not surrounded by pronotal cuticle posteriorly; mesometapectal sulcus crenulate; propodeum carinate. — **Fore wing** hyaline and covered with microtrichiae, two thirds of body length (length 2.57 mm); pterostigma reduced; C, Sc+R, M+Cu, A, Rs fully pigmented; R1 extending beyond marginal cell; Rs closing marginal cell in straight line; M pigmented to apex; medial cell small, elongate and rectangular, nearly triangular by side of 1m-cu. — **Legs** with two mesotibial and one metatibial spurs; metacoxa elongate; metafemur and metatibia swollen; metabasitarsus two to three times as long as remaining metatarsomeres; row of comb-like setae along ventral surface of metatibia and metabasitarsus. — **Metasoma** longer than mesosoma (length 1.44 mm); elongate and narrowed at apex; tergites smooth; hypopygium well-developed; ovipositor shorter than metasoma (length 1.33 mm; OL/BL ratio 0.43), sheaths fully preserved, transversely striated.

3.1.1.2. Genus †*Genkyhag* gen. nov.

<https://zoobank.org/482AE45B-D1E0-44E5-8DBA-49E60CB-77D0A>

Type species. †*Genkyhag innebula* sp. nov.

Etymology. Anagram of Ga Hkyeng, meaning red soil in Jinghpaw, from which the term Kachin is derived. Gender masculine.

Diagnosis. Compound eye oval, higher than long; antenna inserted half way between eye and clypeus; flagellomeres cylindrical, subequal in length (Figs 5C, D). Mesosoma less than half body length, shorter than metasoma; mesoscutum hiding pronotum in dorsal view; median mesoscutal sulcus and axillar groove crenulate; parapsidal lines present, parallel to median mesoscutal sulcus and diverging posteriorly; axillae not contiguous medially; mesoscutellum short (Figs 5A, B); propodeum carinate. Fore wing hyaline, with microtrichiae; venation almost fully pigmented, with only Cu nebulous; medial cell trapezoidal and broad; marginal cell closed without bend; R1 extending beyond this cell (Figs 2C, 5A, B, and E). Legs with one mesotibial and two metatibial spurs. Metasoma elongate, fusiform.

Comments. One of the main differences compared to †*Cretolyra* gen. nov. is the presence of one mesotibial and two metatibial spurs (instead of two mesotibial and one metatibial). The presence of two metatibial spurs seems to be an apomorphy among megalyrids with reversion in some fossil taxa (Vilhelmsen et al. 2010a).

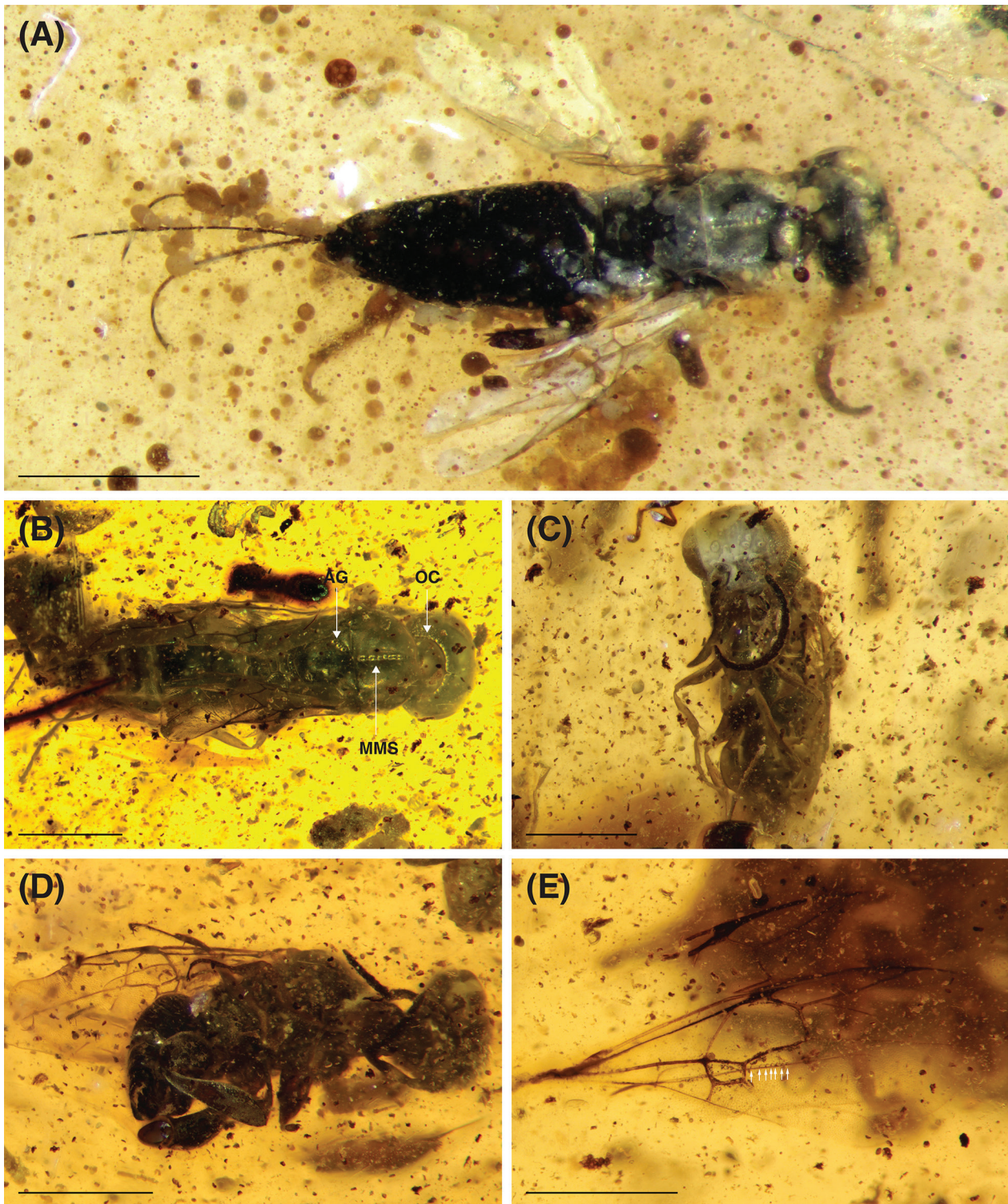


Figure 5. †*Genkyhag innebula* gen. et sp. nov., mid-Cretaceous, Kachin amber. **A** holotype female NIGP203546, habitus in dorsal view; **B** paratype male FAI-BI 11324a, habitus in dorsal view; **C** habitus in frontal view; **D** paratype male FAI-BI 11324b, habitus in lateral view; **E** paratype FAI-BI 11324c, fore and hind wings, with hamuli indicated by arrows. Scale bars: 1 mm (A–E). Abbreviations: AG = inner axillar groove; MMS = median mesoscutal sulcus; OC = occipital carina.

3.1.1.2.1. †*Genkyhag innebula* sp. nov.

<https://zoobank.org/407F2F7B-CA5D-467C-AFF5-11C7A2E9BCDA>

Figures 2C, 5

Etymology. From Latin ‘nebula, In nebula’, meaning “in the fog”, in reference to the amber pieces where the specimens are found, that contains numerous terrigenous inclusions, sometimes partially hiding the specimens. It is a noun in apposition.

Material studied. *Holotype* female NIGP203546; housed in the Nanjing Institute of Geology and Palaeontology (NIGP), Chinese Academy of Sciences, Nanjing, China. Three *paratypes* male FAI-BI 11324a, male FAI-BI 11324b, FAI-BI-11324c of unknown sex; housed in the Fushun Amber Institute.

Type locality. Noije Bum Hill, Hukawng Valley, Kachin State, Myanmar.

Age. Upper Albian to lower Cenomanian, mid-Cretaceous.

Diagnosis. As for genus.

Description. Holotype female incompletely preserved (body length 3.12 mm), in a piece with multiple terrigenous inclusions. Paratypes preserved in a single piece: FAI-BI 11324a visible in dorsal and frontal views, FAI-BI 11324b in lateral view (body length ca. 3.45 mm), FAI-BI 11324c being one complete fore and hind wings and a partial fore wing. — **Head** globular, apparently entirely glabrous (length for holotype ca. 0.47 mm); frons shagreened, convex, divided by a faintly impressed sulcus; compound eye oval, without postocular carina; vertex convex, shagreened; clypeus short; subantennal groove present; toruli inserted half way between clypeus and eyes; antenna short, barely reaching propodeum; scape globular; pedicel slightly longer; flagellomeres cylindrical, longer than wide; flagellomeres 7–11 shorter than flagellomeres 1–6; flagellomere 12 longest; occipital carina crenulate. — **Mesosoma** slightly shorter than metasoma (length for holotype 1.12 mm; for paratype 11324a 1.29 mm; for paratype 11324b 1.57 mm); pronotum not visible dorsally; mesoscutum shagreened, half as long as mesosoma, median mesoscutal sulcus crenulate (mesoscutum length for holotype 0.51 mm; for paratype 11324a 0.61 mm; width for holotype 0.65 mm; for paratype 11324a 0.71 mm); parapsidal lines present; axillae barely contiguous medially and inner grooves crenulate; mesoscutellum wider than long, shorter than mesoscutum; pronotum smooth, not visible dorsally, with posteromedial part moderately high as viewed laterally; anterior thoracic spiracle not fully surrounded by pronotal cuticle; propodeum carinate, carinae delimitating row of small foveae in anterior region and larger foveae in posterior region. — **Fore wing** hyaline, covered with microtrichiae (length for holotype 1.84 mm; for paratype 11324a 2.10 mm; for paratype 11324b 2.11 mm; for paratype 11324c 2.86 mm); venation almost complete, Sc+R, M+Cu, A, Rs+M and M fully pigmented; Cu spectral; marginal cell very narrow, closed in straight line; R1 barely extending beyond marginal cell; medial cell rectangular and relatively broad. — **Hind wing** hyaline; venation reduced to Sc+R and R1, Sc+R almost not diverging from margin, R1 pigmented almost to tip; at least seven hamuli, located distal to middle of hind wing. — **Legs** with one mesotibial and two metatibial spurs; metafemur swollen; ventral surface of metatibia and metabasitarsus with row of comb-like setae, metabasitarsus at least three

times as long as following metatarsomeres. — **Metasoma** elongate, oval, with sparse short setae (length for holotype 1.43 mm); tergites smooth; ovipositor shorter than metasoma (length for holotype 1.34 mm; OL/BL ratio 0.43).

3.1.1.3. Genus †*Megacoxa* gen. nov.

<https://zoobank.org/7AAE84F9-483D-42A6-A210-2C0BB-64CD140>

Type species. †*Megacoxa janzeni* sp. nov.

Etymology. The genus name refers to the size of the metacoxa, which is the key diagnostic feature of the genus; besides, the prefix *Mega-* alludes to the family name Megalyridae. Gender feminine.

Diagnosis. Compound eye oval; scape wider than long; thin occipital carina slightly crenulate. Parapsidal line present and located on posterolateral part of mesoscutum (Figs 6C, 7B and E); inner axillar groove crenulate (Fig. 8F). Fore wing venation with R1, M+Cu, Sc+R, A and Cu fully pigmented; A connected to medial cell with cu-a; Rs closing marginal cell without bend (Figs 2D–F). Metacoxa much enlarged, with dorsal surface rounded to angular, outer metacoxal surface posteriorly foveate, inner metacoxal surface almost entirely accommodated in anterolateral, shallow concavity of metasoma (Figs 6C, 7B, 8C and G). Metatibia and metabasitarsus with ventral row of comb-like setae; two mesotibial and two metatibial spurs (Figs 6A and 7A). Metasoma slightly shorter than mesosoma, tergites and sternites beveled (Figs 6B and 7A).

Comments. The enlarged metacoxa accommodated in the anterior metasomal concavity is the key diagnostic feature for †*Megacoxa* gen. nov. This condition is present in all five specimens assigned to this genus and the metacoxae are clearly symmetrical in the synchrotron-scanned specimen, thus ruling out a preservational artefact.

3.1.1.3.1. †*Megacoxa chandhrasa* sp. nov.

<https://zoobank.org/E022887A-313B-496D-8AA7-94D8927148C3>

Figures 2D, 6

Etymology. The specific epithet is a noun in apposition. It is the name of the legendary sword of Mañjuśrī, a bodhisattva in Buddhism, which allowed him to open the Kathmandu valley, and refers to the long, sword-like metatibial spurs of this species.

Material studied. *Holotype* female IGR.BU-068; housed in the amber collection of the Geology Department and

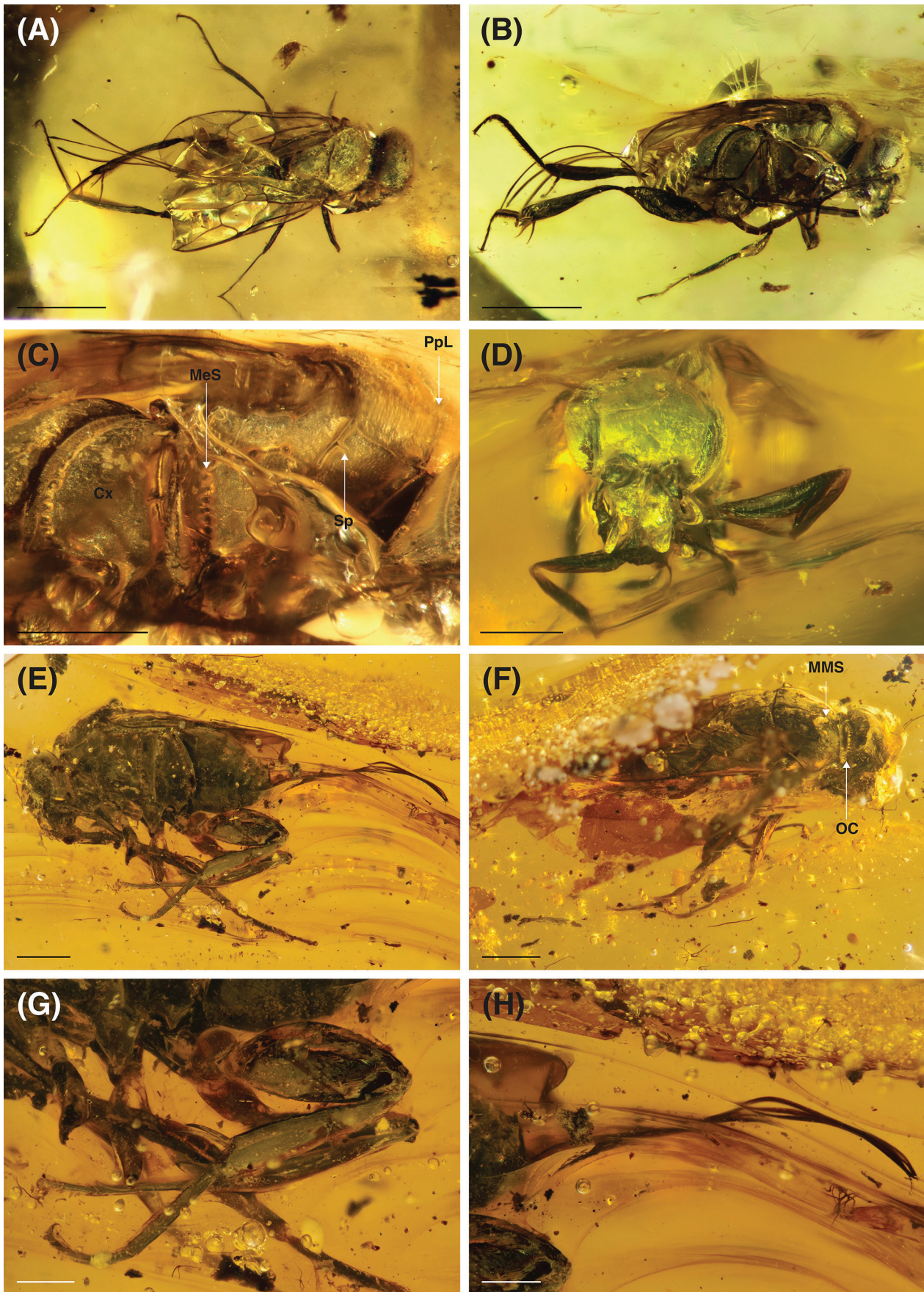


Figure 6. †*Megacoxa chandhrasa* gen. et sp. nov., mid-Cretaceous, Kachin amber. **A** holotype female IGR.BU-068, habitus in dorsal view; **B** habitus in lateral view; **C** mesosoma in lateral view; **D** head in frontal view; **E** paratype female CNU-HYM-MA2016207, habitus in lateral view; **F** head and mesosoma in dorsolateral view; **G** hind legs; **H** ovipositor and its sheaths. Scale bars: 1 mm (**A**, **B**, **E**, **F**); 0.5 mm (**C**, **D**, **G**, **H**). Abbreviations: Cx = hind coxa; MeS = mesometapectal sulcus; MMS = median mesoscutal sulcus; OC = occipital carina; PpL = parapsidal line; sp = anterior thoracic spiracle.

Museum of the University of Rennes, France (IGR). **Paratype** female CNU-HYM-MA2016207; housed in the Key Lab of Insect Evolution and Environmental Changes, College of Life Sciences, Capital Normal University, Beijing, China (CNU).

Type locality. Noiye Bum Hill, Hukawng Valley, Kachin State, Myanmar.

Age. Upper Albian to lower Cenomanian, mid-Cretaceous.

Diagnosis. Median mesoscutal sulcus smooth (Fig. 6F; vs. crenulate in *Megacoxa synchrontron* **gen. et sp. nov.**); axillae contiguous medially (Fig. 6A; vs. separated medially in *Megacoxa janzeni* **gen. et sp. nov.**); medial cell elongate, almost triangular (Figs 2D and 6A; vs. broad and rectangular in *Megacoxa synchrontron* **gen. et sp. nov.** and *Megacoxa janzeni* **gen. et sp. nov.**); posterior margin of metacoxa outcurved and bordered with small foveae (Fig. 6C; vs. bordered with large foveae in *Megacoxa janzeni* **gen. et sp. nov.** and straight posterior metacoxal margin with large foveae in *Megacoxa synchrontron* **gen. et sp. nov.**); metatibial spurs very long (Figs 6A, B and G); metasoma compressed, distinctly shorter than ovipositor; OL/BL ratio ~0.70.

Description. Body length for holotype 2.64 mm; for paratype 4.80 mm. — **Head** globular, higher than long (length for holotype 0.52 mm; for paratype 0.93 mm), glabrous; frons convex, shagreened; compound eye oval, higher than long; vertex convex; clypeus short, shagreened; toruli inserted closer to each other than to eyes; subantennal groove present; antennae distorted, flagellomeres apparently cylindrical, longer than wide; occipital carina crenulate. — **Mesosoma** more than half body length (length for holotype 1.43 mm; for paratype 1.92 mm); covered with short setae; mesoscutum convex, wide (length for holotype 0.62 mm, width for holotype 0.74 mm; length for holotype 0.93 mm, width for holotype 0.90 mm), divided by smooth median mesoscutal sulcus; parapsidal lines present; axillae contiguous medially, inner axillar groove crenulate; pronotum not visible dorsally; anterior thoracic spiracle not fully surrounded by pronotal cuticle; mesometapectal sulcus crenulate; propodeum shorter than mesoscutellum, carinate. — **Fore wing** hyaline and covered with microtrichiae, slightly wrinkled at apex, as long as body (length for holotype 2.08 mm; for paratype 3.52 mm); venation complete with R1, M+Cu, Sc+R, Rs, A and Cu fully pigmented; Rs closing marginal cell; medial cell elongate; A connected to medial cell by 1cu-a. — **Legs** distorted; two mesotibial spurs; metacoxa huge, almost as high anteriorly as maximal propodeal height, with dorsal surface semicircular, posteroventral corner acute, ventral surface notched just anteriorly to trochanter insertion; outer metacoxal surface posteriorly with row of small foveae; dense row of short, comb-like setae along ventral surface of metatrochanter (full length), metafemur (basal half length), metatibia (distal half length), and metabasitarsus (full length); metafemur swollen; two long metat-

ibial spurs, about twice as long as maximal tibial width; metabasitarsus three to four times longer than following metatarsomeres. — **Metasoma** relatively short (length for holotype 1.21 mm; for paratype 1.95 mm), distorted, partly intruding into propodeum during fossilization; tergites and sternites inserted in bevel, smooth; ovipositor longer than metasoma (length for holotype 1.87 mm, OL/BL ratio 0.70; length for paratype 3.24 mm, OL/BL ratio 0.68), sheaths transversely striated.

Comments. We first interpreted the very high OL/BL ratio of the holotype of †*Megacoxa chandhrasra* **gen. et sp. nov.** compared to other †Megalavini (0.70 vs. ~0.40) as a distortion of the specimen and the intruding of the metasoma into the mesosoma. However, the discovery of an additional specimen confirms that the metasoma is more compact in this species than in other species of the genus or the subfamily.

3.1.1.3.2. †*Megacoxa janzeni* sp. nov.

<https://zoobank.org/2CA7827C-7E82-434B-939D-E3C2E-C9DD6EE>

Figures 2E and 7

Etymology. The specific epithet is a patronym honoring Jens-Wilhelm Janzen, former owner of the holotype specimen.

Material studied. **Holotype** female IGR.BU-069; housed in the amber collection of the Geology Department and Museum of the University of Rennes, France (IGR). One **paratype** male NIGP203547; housed in the Nanjing Institute of Geology and Palaeontology (NIGP), Chinese Academy of Sciences, Nanjing, China.

Type locality. Noiye Bum Hill, Hukawng Valley, Kachin State, Myanmar.

Age. Upper Albian to lower Cenomanian, mid-Cretaceous.

Diagnosis. Median mesoscutal sulcus smooth (vs. crenulate in *Megacoxa synchrontron* **gen. et sp. nov.**); axillae not contiguous medially (vs. contiguous in †*Megacoxa chandhrasra* **gen. et sp. nov.** and *Megacoxa synchrontron* **gen. et sp. nov.**); fore wing with very narrow marginal cell closed in straight line by Rs (vs. broad with Rs curved in †*Megacoxa chandhrasra* **gen. et sp. nov.**); trapezoid medial cell (Fig. 2E; vs. narrow in †*Megacoxa chandhrasra* **gen. et sp. nov.**); posterior margin of metacoxa outcurved and bordered with large foveae (Fig. 7B; vs. bordered with small foveae in †*Megacoxa chandhrasra* **gen. et sp. nov.** and straight posterior metacoxal margin in *Megacoxa synchrontron* **gen. et sp. nov.**).

Description. Body length for holotype 5.20 mm; for paratype 3.72 mm. — **Head** glabrous, globular, higher than

long (length for holotype 0.81 mm; for paratype 0.69 mm; height for holotype 1.04 mm; for paratype 0.75 mm); compound eye oval, higher than long, ocular carina absent; vertex convex, shagreened; clypeus short; subantennal groove present; antenna short, less than half as long as body; scape as long as wide (length for holotype 0.19 mm); pedicel wider than long (length for holotype 0.12 mm); flagellomeres cylindrical, elongate; mandibles symmetrical, with three teeth; occipital carina minutely crenulate. — *Mesosoma* half as long as body length (length for holotype 2.28 mm; for paratype 1.62 mm); mesoscutum one third as long as mesosoma (length for holotype

0.92 mm; for paratype 0.63 mm; width for holotype 1.03 mm), shagreened, overhanging pronotum almost at right angle, divided by smooth median mesoscutal sulcus; parapsidal line present; axillae not contiguous medially, inner axillar groove crenulate; pronotum with postero-medial part moderately high as viewed laterally; anterior thoracic spiracle not fully surrounded by pronotal cuticle; mesometapectal sulcus crenulate; propodeum carinate. — *Fore wing* hyaline and covered with microtrichiae, about two thirds of body length (length for holotype 3.08 mm; for paratype 2.58 mm); R1, Sc+R and M+Cu pigmented, Rs present between r-rs and Rs+M, composing first sub-

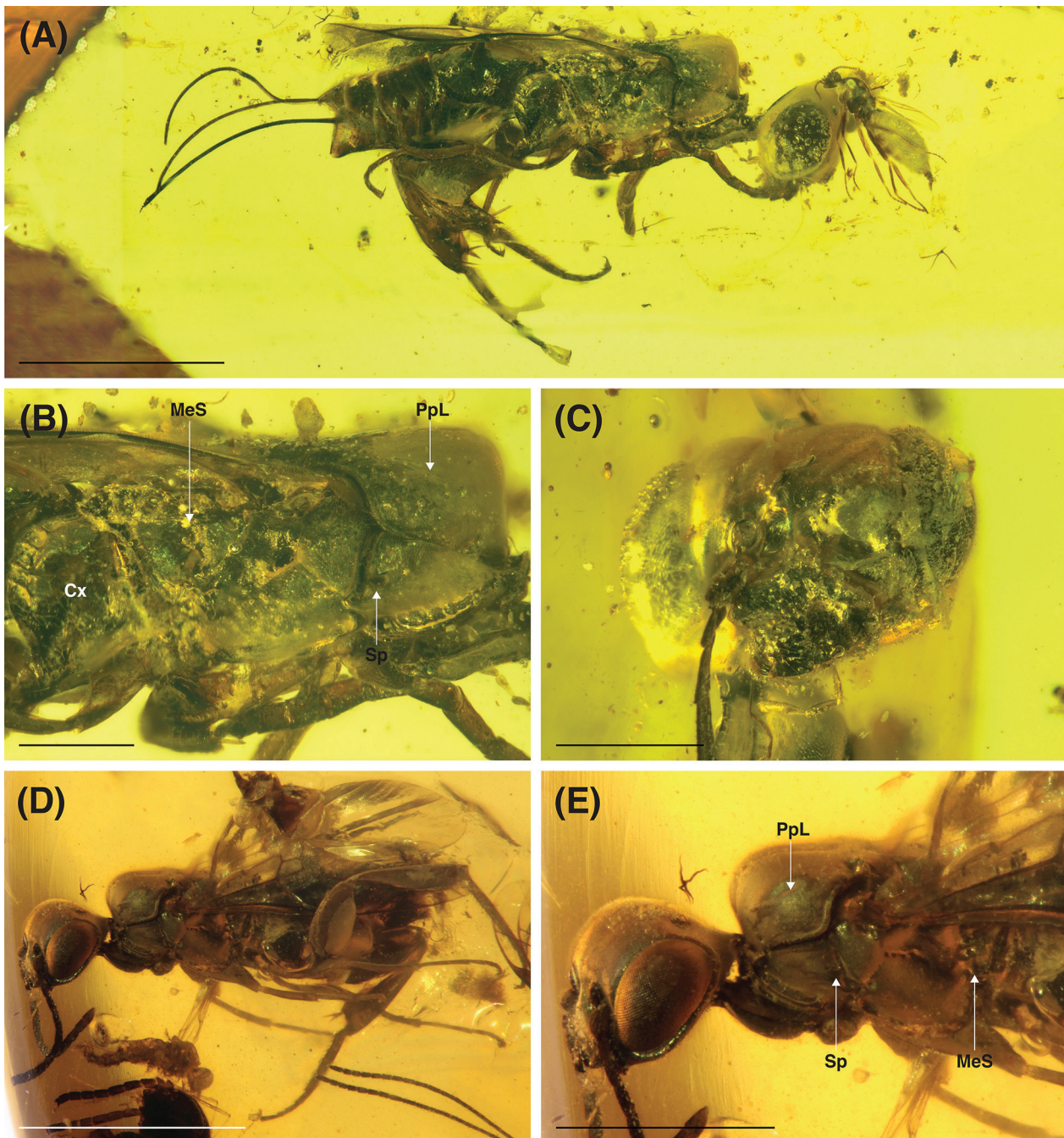


Figure 7. †*Megacoxa janzeni* gen. et sp. nov., mid-Cretaceous, Kachin amber; **A** holotype female IGR.BU-069, habitus in lateral view; **B** mesosoma in lateral view; **C** head in frontal view; **D** paratype male NIGP203547, habitus in lateral view; **E** head and mesosoma in lateral view (scale bars: **A**, **D** = 2 mm; **E** = 1 mm; **B**, **C** = 0.5 mm). Abbreviations: Cx = hind coxa; MeS = mesometapectal sulcus; PpL = parapsidal line; sp = anterior thoracic spiracle.

marginal cell, M and A pigmented, Rs closing in a straight line a very narrow medial cell, trapezoid medial cell composed by basal segments of M, Rs+M and Cu1 (shortest side) and by 1m-Cu, Cu pigmented to margin with a bend. — **Legs** with metacoxa enlarged, posteriorly curved, and notched just before trochanter insertion, bearing a row of large foveae along posterior margin; two mesotibial spurs present; metafemur swollen and bare; metatibia also swollen, with two spurs and bearing row of comb-like setae that continue on metabasitarsus; metatarsus almost as long as metatibia; metabasitarsus four times longer than following metatarsomeres. — **Metasoma** shorter than mesosoma, covered with short setae (length for holotype 2.12 mm; for paratype 1.41 mm); first tergite longest and second almost same length; third, fourth and fifth of similar length and shorter than first; last tergite twice as long as fifth; tergite and sternite inserted in bevel; hypopygium well-developed; ovipositor same length as metasoma (length for holotype 2.10 mm; OL/BL ratio 0.40), sheaths fully preserved in holotype, transversely striated.

3.1.1.3.3. †*Megacoxa synchrotron* sp. nov.

<https://zoobank.org/478CD717-0A9F-4990-94C5-73DD9302F8D4>

Figures 2F and 8

Etymology. The specific epithet is an adjective and refers to the μ -CT technique used at the Deutsches Elektronen-Synchrotron (DESY; Hamburg, Germany) to reconstruct the external surface of the specimen, as well as the internal features for a later study.

Material studied. Holotype male CASENT0753237; housed in the collection of the Phyletisches Museum Jena, Germany (PMJ).

Type locality. Noije Bum Hill, Hukawng Valley, Kachin State, Myanmar.

Age. Upper Albian to lower Cenomanian, mid-Cretaceous.

Diagnosis. Flagellomeres 1–7 distinctly longer than wide; flagellomeres 8–12 slightly longer than wide (Fig. 8A); median mesoscutal sulcus crenulate (vs. smooth in †*Megacoxa chandhrasa* gen. et sp. nov. and †*Megacoxa janzeni* gen. et sp. nov.); axillae contiguous medially (Figs 8D and F; vs. separated medially in †*Megacoxa janzeni* gen. et sp. nov.); fore wing with medial cell wide (Fig. 2F; vs. narrow in †*Megacoxa chandhrasa* gen. et sp. nov.); posterior margin of metacoxa straight, with large foveae (Figs 8C and G; vs. rounded with small foveae in †*Megacoxa chandhrasa* gen. et sp. nov. and rounded with large foveae in †*Megacoxa janzeni* gen. et sp. nov.); comb-like setae reduced on the metabasitarsus (Fig. 8A; vs. more developed on metatibia and metabasitarsus in †*Megacoxa chandhrasa* gen. et sp. nov. and †*Megacoxa janzeni* gen. et sp. nov.).

Description. Body length 2.89 mm. — **Head** globular, higher than long (length 0.45 mm; height 0.53 mm), glabrous; frons convex, shagreened; compound eye oval, higher than long, without postocular carina; vertex convex, shagreened; clypeus short, shagreened; subantennal groove present; antenna filiform, reaching metacoxa; scape short and wide (length 0.09 mm); pedicel thinner than scape, shorter than flagellomeres (length 0.07 mm); flagellomeres cylindrical, elongate; flagellomeres 1–7 distinctly longer than wide (length ca. 0.11–0.14 mm); flagellomeres 8–11 slightly longer than wide (length 0.09 mm); flagellomere 12 longest (length 0.16 mm); mandible with three teeth; occipital carina minutely crenulate. — **Mesosoma** longer than metasoma (length 1.27 mm); mesoscutum (length 0.48 mm) convex, shagreened, divided by crenulate median mesoscutal sulcus; parapsidal lines present; axillae contiguous medially; inner axillar groove crenulate; mesoscutellum diamond-shaped, with blunt posterior margin; pronotum shagreened, with postero-medial part moderately high as viewed laterally; anterior thoracic spiracle not fully surrounded by pronotal cuticle; mesometapetal sulcus crenulate; propodeum carinate, carinae delimiting large fovea on median anterior region, smaller foveae laterally, large foveae on lateral median region and large triangular foveae on posterior region. — **Fore wing** hyaline, uniformly micropubescent (length 2.04 mm); venation complete with R1, Sc+R, M+Cu, A, Rs+M, Rs, M and Cu fully pigmented; Rs+M aligned with M+Cu; medial cell wide; Rs present between Rs+M and r-rs, closing first submarginal cell; marginal cell narrow, closed in straight line by Rs. — **Legs** with metacoxa enlarged, posterior margin straight with upper corner angularly produced, bearing row of large foveae along posterior margin; metafemur and metatibia swollen; two mesotibial and two metatibial spurs; metabasitarsus with row of sparse comb-like setae along ventral margin. — **Metasoma** smooth, fusiform (length 1.17 mm); tergites inserted in bevel.

3.2. Subfamily Megalyrinae Schletterer, 1889

Emended diagnosis. Head globular; compound eye oval, with or without postocular carina; flagellomeres often elongate, sometimes compact; subantennal groove with or without dorsal carina, mandibles symmetrical with three teeth. Anterior thoracic spiracle fully surrounded by pronotal cuticle; median mesoscutal sulcus sometimes effaced or reduced; parapsidal lines sometimes absent. Fore wing with infumate banding patterns in *Ettchellsia*, *Dinapsis*, *Megalyra* and *Megalyridia*; at least Sc+R, Rs+M, basal segment of Rs and basal segment of R1 pigmented and no closed cell; at most with C, Sc+R, A, cu-a, Rs+M, Rs, R1 and basal segment of M pigmented, costal, submarginal, and marginal cells closed by tubular veins, subcostal and first cubital fused; M+Cu usually absent except in †*Cretodinapsis*; rarely brachypterous. Hind leg without row of erect setae along margin. Metasoma usually elongate but sometimes distinctly shorter than mesosoma.

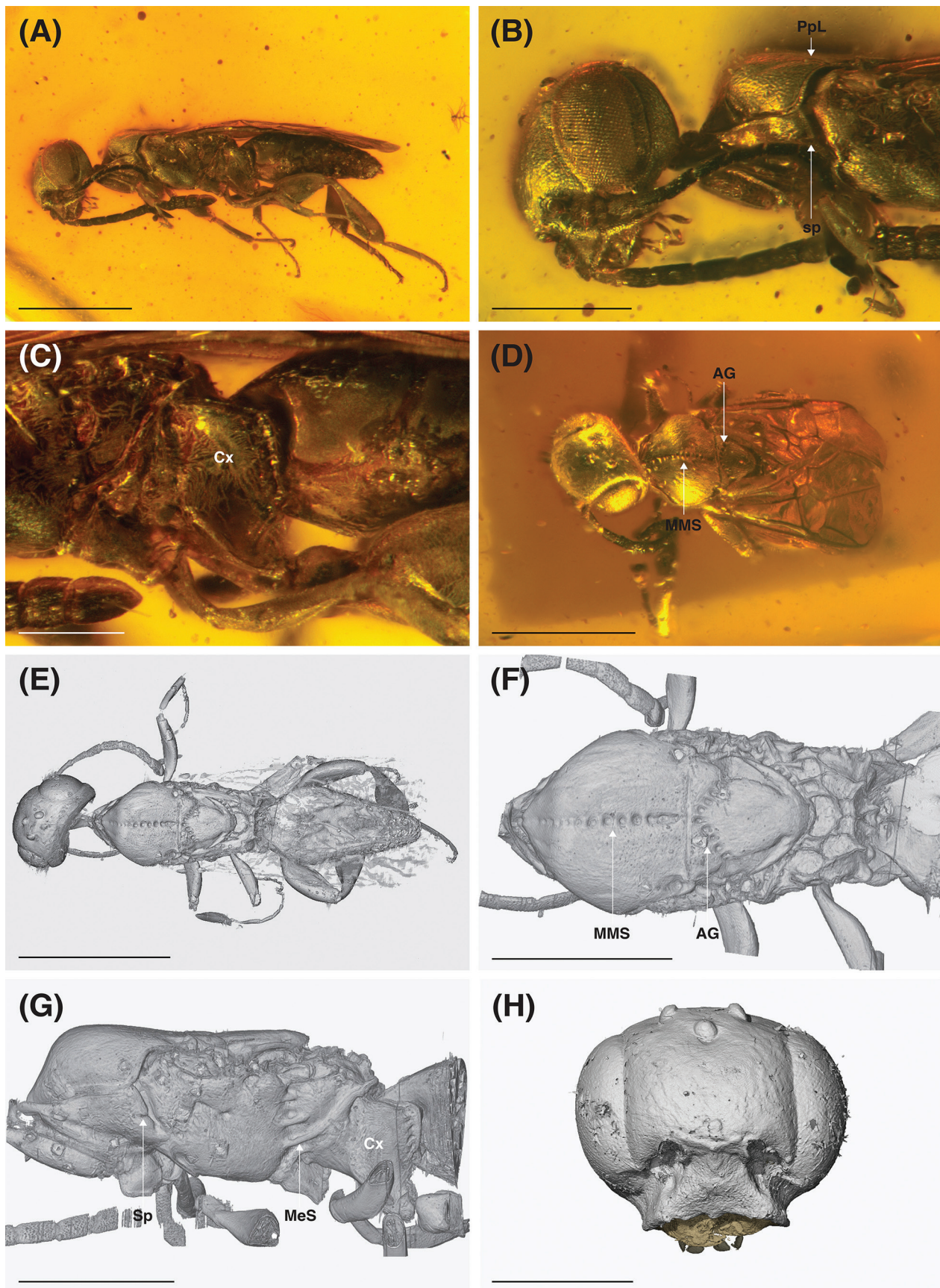


Figure 8. †*Megacoxa synchrotron* gen. et sp. nov., holotype male CASENT0753237, mid-Cretaceous, Kachin amber (**E–H**: reconstructed using synchrotron radiation-based micro-computed tomography). **A** habitus in lateral view; **B** head and anterior mesosoma in lateral view; **C** metacoxa in lateral view; **D** habitus in dorsal view; **E** habitus in dorsal view; **F** mesosoma in dorsal view; **G** mesosoma in lateral view; **H** head in frontal view, with antennae numerically removed. Scale bars: 1 mm (**A**, **D**, **E**); 0.5 mm (**B**, **F**, **G**, **H**); 0.25 mm (**C**). Abbreviations: AG = inner axillar groove; Cx = hind coxa; MeS = mesometapetal sulcus; MMS = median mesoscutal sulcus; PpL = parapsidal line; sp = anterior thoracic spiracle.

Genera included. *Carminator* Shaw, 1988, *Cryptalyra* Shaw, 1987 [Cryptalyrini Shaw, 1988]; *Dinapsis* Waterston, 1922, *Ettchellsia* Cameron, 1909, *Neodinapsis* Shaw, 1987 [Dinapsini Waterston, 1922]; †*Cretodinapsis* Rasnitsyn, 1977, *Megalyra* Westwood, 1832, †*Prodinapsis* Brues, 1923 [Megalyrini Schletterer, 1889]; †*Kamyristi* **gen. nov.** [†*Kamyristini* **trib. nov.**]; *Megallica* Perrichot, 2009 [†*Megallicini* **trib. nov.**]; *Megalyridia* Hedqvist, 1959 [Megalyridiini Shaw, 1990]; *Rigel* Shaw, 1987 [Rigelini Shaw, 1990]; †*Valaa* Perrichot, 2009 [†*Valaaini* **trib. nov.**].

Stratigraphic extension. Albian to present.

Comments. We redefine the subfamily Megalyrinae, according to the results of the phylogenetic analyses. The subfamily is composed of three non-monotypic tribes, namely Cryptalyrini, Dinapsini, and Megalyrini, as well as a number of monotypic tribes: Rigelini, †*Kamyristini* **trib. nov.**, †*Megallicini* **trib. nov.**, †*Valaaini* **trib. nov.**, and Megalyridiini. The justification for redefining Megalyrinae is given in the Discussion.

3.2.1. Tribe †*Kamyristiini* **trib. nov.**

Type genus. †*Kamyristi* **gen. nov.**

Diagnosis. Head prognathous; compound eye without setation, without posterior carina; subantennal groove without dorsal carina; mandible with three teeth; occipital carina present, curving towards mandible. Median mesoscutal sulcus crenulate; parapsidal line absent; propodeum areolate-rugose. Fore wing hyaline with C, Sc+R, A, cu-a, Rs+M, M, Rs and R1 tubular; pterostigma large; M not reaching apical margin; Rs only present as a stub between Rs+M and r-rs; Rs apically strongly angled, arched towards stigma; Metasoma elongate, fusiform, longer than mesosoma; ovipositor sheaths only covering basal portion of ovipositor.

Genera and species included. †*Kamyristi exfrigore* **gen. et sp. nov.**, †*Kamyristi yantardakhensis* **gen. et sp. nov.**

Comments. The tribe †*Kamyristiini* **trib. nov.** is erected based on the results of the phylogenetic analyses, to accommodate †*Kamyristi* **gen. nov.** and its two species. †*Kamyristi* **gen. nov.** is not retrieved within a larger clade, precluding its assignment to another monophyletic tribe.

3.2.1.1. Genus †*Kamyristi* **gen. nov.**

<https://zoobank.org/62D92992-92DA-47CE-B987-C8B-D825EBBF8>

Type species. †*Kamyristi exfrigore* **sp. nov.**

Etymology. Anagram of Taïmyrski, the Russian name of the Taimyr peninsula from where the amber pieces containing the specimens derive. Gender masculine.

Diagnosis. As for tribe with the following additional characters: head shagreened; compound eye higher than long; occipital carina foveate (Figs 9C and F); flagellomeres cylindrical and elongate. Mesosoma less than half of metasoma length; mesoscutum reduced on anterior part of mesosoma, hiding pronotum dorsally (Figs 9B and F). Fore wing with medial cell pentagonal with 1m-cu, Cu1 and M+Cu and Cu spectral, Rs+M not aligned with M+Cu (Figs 2G, H, 9B and D). Hind leg with scattered erect setae; one mesotibial and one metatibial spur.

Comments. Two species from this genus are known, both displaying numerous similarities with the extant genus *Cryptalyra* from South America, e.g., the elongate smooth metasoma (Fig. 9A), the erect setae on the hind leg (Fig. 9A) or M half pigmented (Figs 2G and H). But †*Kamyristi exfrigore* **gen. et sp. nov.** displays the most surprising affinities to *Cryptalyra*: the ovipositor sheaths seem very reduced, only covering the basal part of the ovipositor (Fig. 9A). However, the closed marginal cell (Fig. 2G and H), the elongate flagellomeres (Fig. 9E) and the mesosoma being shagreened instead of foveate (Fig. 9C) indicate that it is not closely related to *Cryptalyra*. Examination of more female specimens will be necessary to confirm if reduced ovipositor sheaths are a diagnostic character for this genus. †*Kamyristi* **gen. nov.** species are the smallest megalyrids in Asia.

Due to the fore wing venation and absence of a sulcus on the vertex, this new genus resembles Dinapsini with Rs reduced. Another difference is the posterior head sculpture, distinctly shagreened, whereas it is reticulate for the extant dinapsine species. Finally, the lack of grooves behind the eyes and of a dorsal carina on the subantennal groove makes the placement in Dinapsini doubtful; they are similarly absent in †*Valaa delclosi*. According to Shaw (1990a), these characters are relatively homoplasious. The placement of †*Kamyristi* **gen. nov.** in the Dinapsini is not corroborated by the phylogenetic analyses (see below).

3.2.1.1.1. †*Kamyristi exfrigore* **sp. nov.**

<https://zoobank.org/2141EC6A-4F85-4ECA-A118-0F3F-8CBF1D34>

Figures 2G, 9A–C

Etymology. “*exfrigore*” means “from the cold” in Latin as this species is the northernmost record of a megalyrid, extant and extinct, in a region where the temperature is currently below zero most of the year. The specific epithet is to be treated as an adjective.

Material studied. *Holotype* female PIN 3730/411; housed in the collection of the Paleontological Institute of the Russian Academy of Sciences (PIN).

Type locality. Baikura, Russia.

Age. Upper Albian to lower Cenomanian, mid-Cretaceous.

Diagnosis. Eye nearly round (vs. oval, higher than long in †*Kamyristi yantardakhensis* gen. et sp. nov.); axillae contiguous medially with axillar groove smooth (Fig. 9B; vs. separated medially with axillar groove crenulated in †*Kamyristi yantardakhensis* gen. et sp. nov.).

Description. Body length 2.03 mm. Almost complete, except ovipositor. — **Head** globular, higher than long (length 0.38 mm; height 0.43); slightly pubescent on

vertex and frons; frons convex, shagreened; compound eye rounded, slightly higher than long, not covering head length, postocular carina absent; vertex convex, shagreened; torulus inserted very close to ventral margin of eye; subantennal groove present; mandible with three teeth; scape short and thick (length 0.09 mm); pedicel same length; flagellomeres cylindrical, longer than wide, elongate (length ca. 0.08 mm); flagellomere 12 longest; occipital carina crenulate. — **Mesosoma** shorter than metasoma (length 0.69 mm; height 0.40 mm), almost fully shagreened; mesoscutum shagreened, short (length 0.20 mm; width 0.47 mm), one third of mesosoma length,

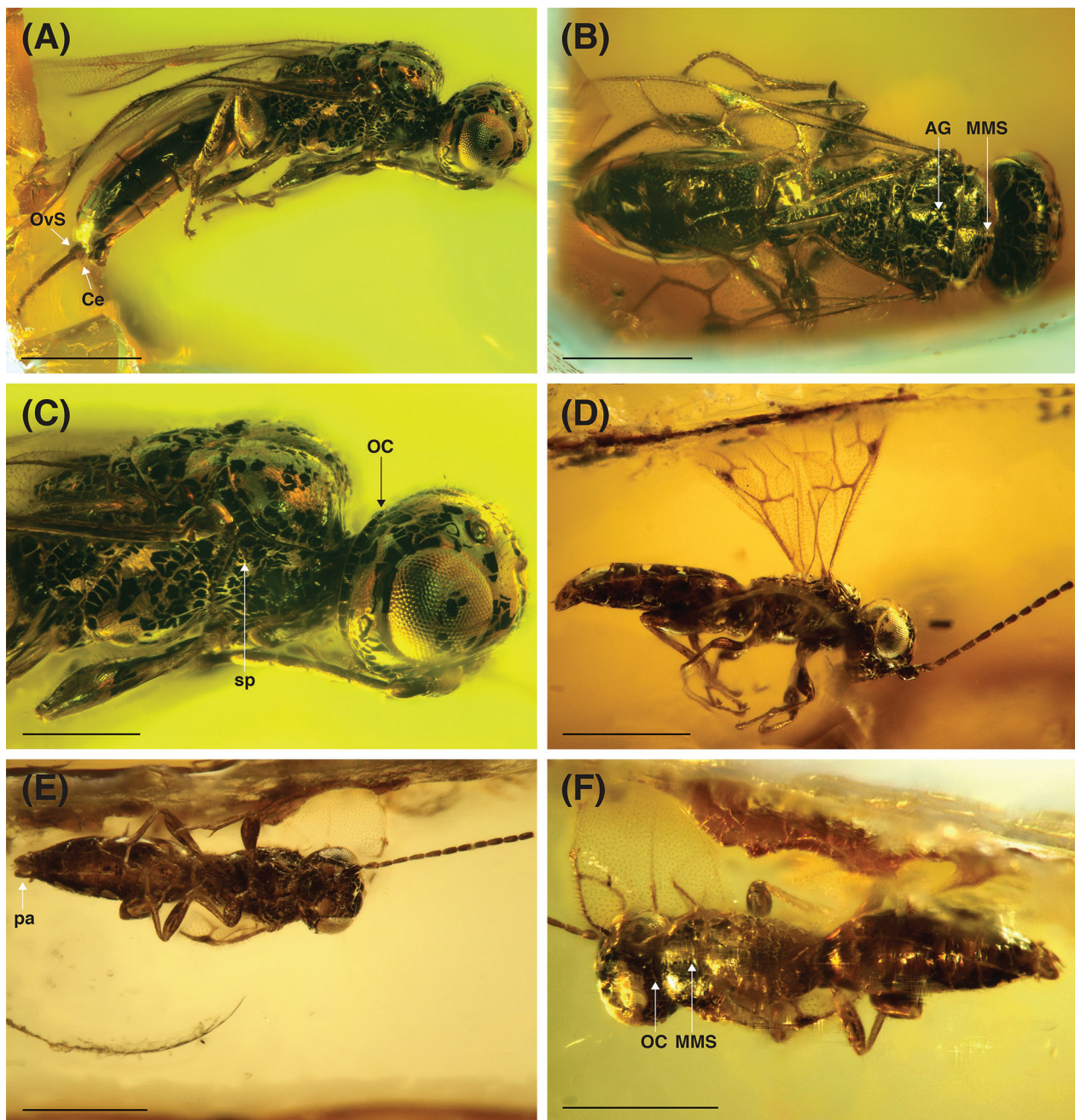


Figure 9. †*Kamyristi* gen. nov. **A–C** †*Kamyristi exfrigore* gen. et sp. nov., holotype female PIN 3730/411, Albian-Cenomanian, Taimyr amber. **A** habitus in lateral view; **B** habitus in dorsal view; **C** head and mesosoma in lateral view; **D–F** †*Kamyristi yantardakhensis* gen. et sp. nov., holotype male 3311/2718, Santonian, Taimyr amber; **D** habitus in lateral view; **E** habitus in ventral view; **F** habitus in dorsal view. Scale bars: 0.5 mm (**A**, **B**, **D**, **E**); 0.25 mm (**C**). AG = inner axillar groove; ce = cercus; MMS = median mesoscutal sulcus; OC = occipital carina; OvS = ovipositor sheaths; pa = parameres; sp = anterior thoracic spiracle.

divided by crenulate median mesoscutal sulcus, with sparse erect setae; axillae continuous medially, with inner axillar groove smooth; mesoscutellum as long as mesoscutum, posterior margin slightly outcurved; pronotum not visible dorsally; anterior thoracic spiracle fully surrounded by pronotal cuticle; propodeum areolate-rugose. — **Fore wing** hyaline (length ca. 1.50 mm) and covered with microtrichia; C, Sc+R, Rs +M, basal segments of Rs and M; M+Cu, Cu and 1m-cu spectral; Rs not closing first submarginal cell and pigmented for two thirds between r-rs and Rs+M; M pigmented to level of 2r-m and then spectral to wing tip; pterostigma broad; R1 extending beyond marginal cell; Rs pigmented, arched toward stigma, closing marginal cell. — **Legs** bearing many scattered erect setae; one mesotibial spur, one metatibial spur present; metafemur swollen, metatibia notched before spur; metabasitarsus three times longer than following, remainder same length. — **Metasoma** almost half body length (length 0.96 mm), elongate, smooth; segments subequal in length; hypopygium well-developed, concave; ovipositor incomplete, covered by sheaths only at base; cerci triangular, exerted.

3.2.1.1.2. †*Kamyristi yantardakhensis* sp. nov.

<https://zoobank.org/EE93DF47-0E9D-47CA-B231-7997C067D85F>

Figures 2H, 9D–F

Etymology. The specific epithet refers to the locality where the specimen was collected. The specific adjective is to be treated as a noun in a genitive case.

Material studied. *Holotype* male PIN 3311/2718; housed in the collection of the Paleontological Institute of the Russian Academy of Sciences (PIN).

Type locality. Yantardakh, Russia.

Age. Santonian, Upper Cretaceous.

Diagnosis. Axillae not contiguous medially, grooves crenulated (Fig. 9F; vs. contiguous medially, with axillar grooves smooth in †*Kamyristi exfrigore* gen. et sp. nov.).

Description. Body length 1.47 mm. Body mostly bare. — **Head** slightly higher than long (length 0.26 mm; height 0.28 mm), glabrous; frons convex, shagreened; compound eye almond-shaped, higher than long, not covering head length, postocular carina absent; vertex convex, minutely shagreened but sculpture not fully visible; toruli inserted closer to each other than to eyes; subantennal groove present; mandible with three teeth, decreasing in size from apex to base; scape short and thick (length 0.07 mm), pedicel of similar length with scape but thinner; 10 flagellomeres preserved, cylindrical, elongate, longer than wide; flagellomere 1 shortest flagellomere (length 0.04 mm), flagellomeres 2–10 similar in length

(length ca. 0.06 mm); flagellomere 11–12 missing; occipital carina crenulate. — **Mesosoma** more than a third of body length (length 0.43 mm; height 0.22 mm); mesoscutum less than one third of mesosoma length (length 0.15 mm; width 0.31 mm), shagreened and divided by crenulate median mesoscutal sulcus; axillae not continuous medially, with inner groove crenulate; mesoscutellum shagreened; pronotum not visible dorsally; anterior thoracic spiracle fully surrounded by pronotal cuticle; propodeum areolate-rugose. — **Fore wing** hyaline and covered with microtrichia (length ca. 0.75 mm); C, Sc+R, A, Rs and basal segment of M pigmented; M+Cu, Cu and 1m-cu spectral; Rs+M not aligned with M+Cu; medial cell pentagonal; Rs almost closing submarginal cell, not fully pigmented between r-rs and Rs+M; R1 pigmented beyond marginal cell; marginal cell closed by Rs with a bend; M pigmented halfway to wing tip and then spectral. — **Legs** bearing numerous scattered setae; one long mesotibial spur, one shorter metatibial spur; basimetatrotchanter long, half metacoxa length; metafemur slightly swollen; first metatarsomere longest and bearing small erect setae. — **Metasoma** almost half body length, longer than mesosoma (length 0.75 mm), elongate; smooth and bare; tergites nearly equal in length; hypopygium small, parameres triangular, projecting downward.

3.2.2. Tribe †*Megallicini* trib. nov.

Type genus. †*Megallica* Perrichot, 2009.

Diagnosis. Head hypognathous; compound eye without setation, without posterior carina; subantennal groove without dorsal carina; mandible with three teeth; median sulcus on vertex present; occipital carina present, curving towards mandible. Median mesoscutal sulcus crenulate; parapsidal lines absent; axillae not connected at inner angles, separated by two triangular foveae; propodeum areolate-rugose. Fore wing hyaline; with C, Sc+R, A, cu-a, Rs+M, M, Rs and R1 tubular; pterostigma large; M not reaching apical margin; Rs only present as a stub between Rs+M and r-rs; Rs apically evenly arched towards stigma; costal, marginal and radial+first cubital cells closed. Metasoma elongate, fusiform, longer than mesosoma.

Genera and species included. †*Megallica parva* Perrichot, 2009

Comments. The tribe *Megallicini* trib. nov. is erected based on the results of the phylogenetic analyses, because *Megallica* is not retrieved within a clade with any other Megalyrinae genera.

3.2.3. Tribe *Megalyrini* Schletterer, 1889

Cretodinapsini Rasnitsyn, 1977 **syn. nov.**

Prodinapsini Shaw, 1990b

Type genus. *Megalyra* Westwood, 1832.

Emended diagnosis. Head hypognathous; compound eye often with distinct setation; flagellomeres elongate; median sulcus on vertex present; occipital carina present, curving towards mandible. Parapsidal lines absent. Fore wing with C, Sc+R, 1A, Rs+M, basal segment of M, R1, r-rs and small segment of Rs tubular. Metasoma elongate, subcylindrical, longer than mesosoma.

Genera and species included. †*C. caucasica* Rasnitsyn, 1977, *M. aquilonia* Shaw, 1990, *M. australia* Girault, 1925, †*M. baltica* Poinar & Shaw, 2007, *M. brevicauda* Shaw, 1990, *M. caledonica* Vachal, 1908, *M. candata* Szépligeti, 1902, *M. exigua* Shaw, 1990, *M. fasciipennis* Westwood, 1832, *M. globula* Shaw, 1990, *M. gnoma* Shaw, 1990, *M. lilliputiana* Turner, 1916, *M. longiseta* Szépligeti, 1902, *M. minuta* Froggatt, 1906, *M. nanella* Shaw, 1990, *M. plana* Shaw, 1990, *M. pygmaea* Shaw, 1990, *M. reiki* Shaw, 1990, *M. rufipes* Erichson, 1841, *M. rufiventris* Szépligeti, 1902, *M. sedlaceki* Shaw, 1990, *M. shuckardi* Westwood, 1851, *M. spectabilis* Shaw, 1990, *M. tawiensis* Petersen, 1966, *M. testaceipes* Turner, 1916, *M. transversistriata* Girault, 1925, *M. troglodytes* Naumann, 1987, *M. viridescens* Froggatt, 1906, *M. wagneri* Fahringer, 1928, †*P. bruesi* (Perrichot, 2009), †*P. janzeni* Perrichot, 2009, †*P. minor* Brues, 1933, †*P. oesiensis* Perrichot, 2009, †*P. prolata* (Perrichot & Perkovsky, 2009), †*P. pumilio* Perrichot & Perkovsky, 2009, †*P. succinalis* Brues, 1923.

Comments. The tribe Megalyrini is expanded based on the results of the phylogenetic analyses. The genus †*Cretodinapsis* is retrieved to be sister of *Megalyra*, rendering the

†*Cretodinapsis* paraphyletic. Therefore, †*Cretodinapsis* is synonymized with Megalyrini, with †*Cretodinapsis* and †*Prodinapsis* now components of the latter tribe.

3.2.4. Tribe †*Valaaini* trib. nov.

Type genus. †*Valaa* Perrichot, 2009.

Diagnosis. Head hypognathous; compound eye without setation, without posterior carina; subantennal groove without dorsal carina; mandible with three teeth; occipital carina present, curving towards mandible. Median mesoscutal sulcus crenulate; parapsidal lines absent; axillae not connected at inner angles, separated by two triangular foveae; propodeum carinate. Protibia with stout apical spines; pro-, meso- and metatibiae shorter than combined length of tarsomeres. Fore wing hyaline, with C, Sc+R, A, Rs+M, cu-a, Rs, M and R1 tubular; pterostigma reduced; M not reaching apical margin; Rs apically strongly angled, arched towards stigma; costal, submarginal, marginal and radial+first cubital cells closed. Hind wing with Rs short, barely projecting beyond R1. Metasoma compact, shorter than mesosoma.

Genera and species included. †*Valaa delclosi* Perrichot, 2009

Comments. The tribe †*Valaaini* trib. nov. is erected based on the results of the phylogenetic analyses, because †*Valaa* is not retrieved within a clade with other Dinapsini s.s., contrary to what was suggested by Perrichot (2009).

3.3. Key to the genera of Megalyridae

Following the large expansion of the fossil record in the present contribution, we provide an updated key to extant and extinct genera of Megalyridae.

- 1 Anterior thoracic spiracle not surrounded by pronotal cuticle posteriorly (Fig. 3D); fore wing with M+Cu pigmented (Figs 2 and 3C); hind legs with comb-like spines along the inner margin [†*Megazarinae* stat. nov.]2
- 1' Anterior thoracic spiracle fully surrounded by pronotal cuticle; fore wing with M+Cu absent or spectral; hind legs without comb-like spines [Megalyrinae]6
- 2 Occipital carina smooth; fore wing with the medial cell pentagonal; mesometapectal sulcus not crenulate; mandibles with four teeth (Perrichot 2009: figs 15 and 16)..... †*Megazar* Perrichot, 2009
- 2' Occipital carina foveate; fore wing with the medial cell rectangular (Figs 2 and 3C); mesometapectal sulcus crenulate; mandibles with three teeth.....3
- 3 Vertex with a distinct longitudinal median sulcus (Pérez-de la Fuente et al. 2012: fig. 2A; Perrichot 2009: fig. 17.1) †*Megalava* Perrichot, 2009
- 3' Vertex without sulcus4
- 4 Two mesotibial and one metatibial spurs present †*Cretolyra* gen. nov.
- 4' Count of tibial spurs different5
- 5 Presence of two mesotibial and two metatibial spurs; metacoxa enlarged posteriorly with a row of foveae posteriorly (Figs 6B and D) †*Megacoxa* gen. nov.
- 5' Presence of one mesotibial and two metatibial spurs; metacoxa not enlarged posteriorly †*Genkyhag* gen. nov.
- 6 Fore wing with vein Rs+M spectral (Rasnitsyn 1977: fig. 7) †*Cretodinapsis* Rasnitsyn, 1977
- 6' Fore wing with vein Rs+M pigmented7
- 7 Fore wing with vein Rs tubular between Rs+M and r-rs, at least for a short distance8
- 7' Fore wing with vein Rs absent, spectral between Rs+M and r-rs (Perrichot 2009: figs 1.1–1.7; Shaw 1987: fig. 5)14

- 8 Fore wing with vein Rs interrupted between Rs+M and r-rs9
- 8' Fore wing with vein Rs fully pigmented between Rs+M and r-rs, closing the first submarginal cell (Waterston 1922: plate 11; Shaw 1987: fig. 6)11
- 9 Vertex with a distinct longitudinal median sulcus (Perrichot 2009: figs 19.1 and 20.2) ...†*Megallica* Perrichot, 2009
- 9' Vertex without sulcus10
- 10 Fore wing with vein Rs apically nebulous, straight (Vilhelmsen et al. 2010a: fig. 5A)*Rigel* Shaw, 1987
- 10' Fore wing with Rs arched toward stigma, tubular (Figs 6G and H)†*Kamyristi* gen. nov.
- 11 Posterior orbital groove/carina absent; subantennal groove without dorsal carina (Perrichot 2009: fig. 18).....
- †*Valaa* Perrichot, 2009
- 11' Posterior orbital groove/carina present; subantennal groove with a dorsal carina (Vilhelmsen et al. 2010a: figs 2A, B and E).....12
- 12 Posterior orbital groove foveate; fore wings veins 1m-cu and Cu1 absent.....13
- 12' Posterior orbital groove not foveate or reduced to the dorsal portion; fore wings veins 1m-cu and Cu1 present as nebulous to tubular segment (Chen et al. 2021: fig. 4D)*Ettchellsia* Cameron, 1909
- 13 Fore wing vein A present distally of 1cu-a, at least a darkened line; metacoxa with a longitudinal carina; metasoma compact, < 0.40 × BL (Shaw and van Noort 2009: fig. 2F)..... *Dinapsis* Waterston, 1922
- 13' Fore wing vein A absent distally of 1cu-a ; metacoxa without longitudinal carina; metasoma elongate, > 0.45 × BL (Shaw, 1987: figs 3 and 6).....*Neodinapsis* Shaw, 1987
- 14 Vertex with a longitudinal sulcus distinct or at least faintly impressed (Perrichot 2009: figs 2–13).....
- †*Prodinapsis* Brues, 1923
- 14' Vertex without a longitudinal sulcus15
- 15 Flagellomeres compact, at most 1.5 times longer than wide (Vilhelmsen et al. 2010a: fig. 2G); fore wing R1 absent; hind wing Rs absent (Mita and Konishi 2011: figs 14, 15 and 27–28).....16
- 15' Flagellomeres elongate, at least 2 times longer than wide; fore wing R1 present; hind wings Rs present17
- 16 Pterostigma absent; metacoxa shagreened; metatibia with two apical spurs (Shaw, 1988: fig. 1)*Carminator* Shaw, 1988
- 16' Pterostigma present, only swelling at junction with Rs; metacoxa areolate-rugose; metatibia with one apical spur (Kawada et al. 2014: fig. 2).....*Cryptalyra* Shaw, 1987
- 17 Head and mesosoma shagreened; face with a distinct short longitudinal median groove; pronotal spiracle without internal fringe of setae; metacoxa shagreened; metatibia with two apical spurs (van Noort and Shaw 2009: figs 2A–F)*Megalyridia* Hedqvist, 1959
- 17' Head and mesosoma coarsely foveate-reticulate; face without median groove; pronotal spiracle with an internal fringe of setae; metacoxa rugose; metatibia with only one apical spur (Shaw 1990b: figs 16, 18 and 28).....
-*Megalyra* Westwood, 1832

4. Results

4.1. Character list

The character list presented in the Appendix S2 is an expanded version of the dataset of Vilhelmsen et al. (2010a) which comprised 48 characters (indicated as n*). The dataset of Mita and Konishi (2011) has also been explored as a source of potential characters but given the taxonomic rank studied (the genus *Carminator*), only three characters have been included here (indicated as n†). Character 41 has been added as it appears that state 1 of this character is the main apomorphy of the †Megalavini. Due to the inclusion of fewer outgroup taxa in the present paper compared to Vilhelmsen et al. (2010a), characters 9, 23 and 47 in the previous analyses became uninformative and have been deleted.

4.2. Parsimony analyses

Despite different k constants, the analyses produced the same most parsimonious tree (Fig. 10). However, subse-

quent bootstrap analyses run with traditional search for 1000 replications showed that most nodes of the tree were poorly supported. These analyses only supported a few clades with sufficient robustness: †*Kamyristi* gen. nov. (94%), (*Ettchellsia* + *Dinapsis*) (92%) and (*Carminator* + *Cryptalyra*) (83%). The sister group relationships of *Ettchellsia* + *Dinapsis*, and *Carminator* + *Cryptalyra*, respectively, were also retrieved by Vilhelmsen et al. (2010a). Additionally, the monophyly of the Megalyridae is strongly supported (94%); both †Megazarinae stat. nov. and Megalyrinae are retrieved as monophyletic. *Rigel* is sister to all other Megalyrinae; †*Kamyristi* gen. nov., †*Megallica* and †*Valaa* split off in succession from the remaining Megalyrinae. The Dinapsini sensu Perrichot (2009) is not retrieved as monophyletic, but with the exclusion of †*Valaa* the remaining extant Dinapsini form a clade (*Neodinapsis* + (*Dinapsis* + *Ettchellsia*)) that is sister to *Megalyridia* + ((*Cryptalyra* + *Carminator*) + (†*Prodinapsis* + (†*Cretodinapsis* + *Megalyra*))). Finally, one of the most interesting results of these analyses is to find the tribe Cretodinapsini paraphyletic with regard to Megalyrini, with †*Cretodinapsis* as the sister of *Megalyra*. Even when excluding a rogue taxon (i.e.,

†*Cretodinapsis*, 53% missing data), the results of the parsimony analyses are totally congruent (Fig. 11).

4.3. Bayesian analyses

Stepping stone sampling estimated mean marginal likelihoods of -521.77 and -517.98 for the Mk_v for the Mk_v+G models, respectively. Bayes factor comparison ($2\ln_c(H_{01})$) indicates that the statistical significance between these results is negligible ($BF < 1$). In both sets of topology searches, i.e., using Mk_v (Fig. 12) and Mk_v+G

(Fig. 13), the Megalyridae are supported as monophyletic (Bayesian posterior probability, BPP > 0.98). At the subfamily level, only Megalyrinae are recovered under the Mk_v model (BPP ~ 0.77), while only †Megazarinae **stat. nov.** are recovered under the Mk_v+G model (BPP ~ 0.84). Support for relationships between genera is limited, although both models recovered monophyly for †*Kamyristi gen. nov.* (BPP ≥ 0.93), *Dinapsis* + *Ettchellsia* (BPP ≥ 0.99), and *Carminator* + *Cryptalyra* (BPP > 0.94), similarly to the parsimony analyses. Under the variable rates model, *Megacoxa gen. nov.* + †*Cretolyra gen. nov.* is supported as a clade (Mk_v+G BPP ~ 0.54)

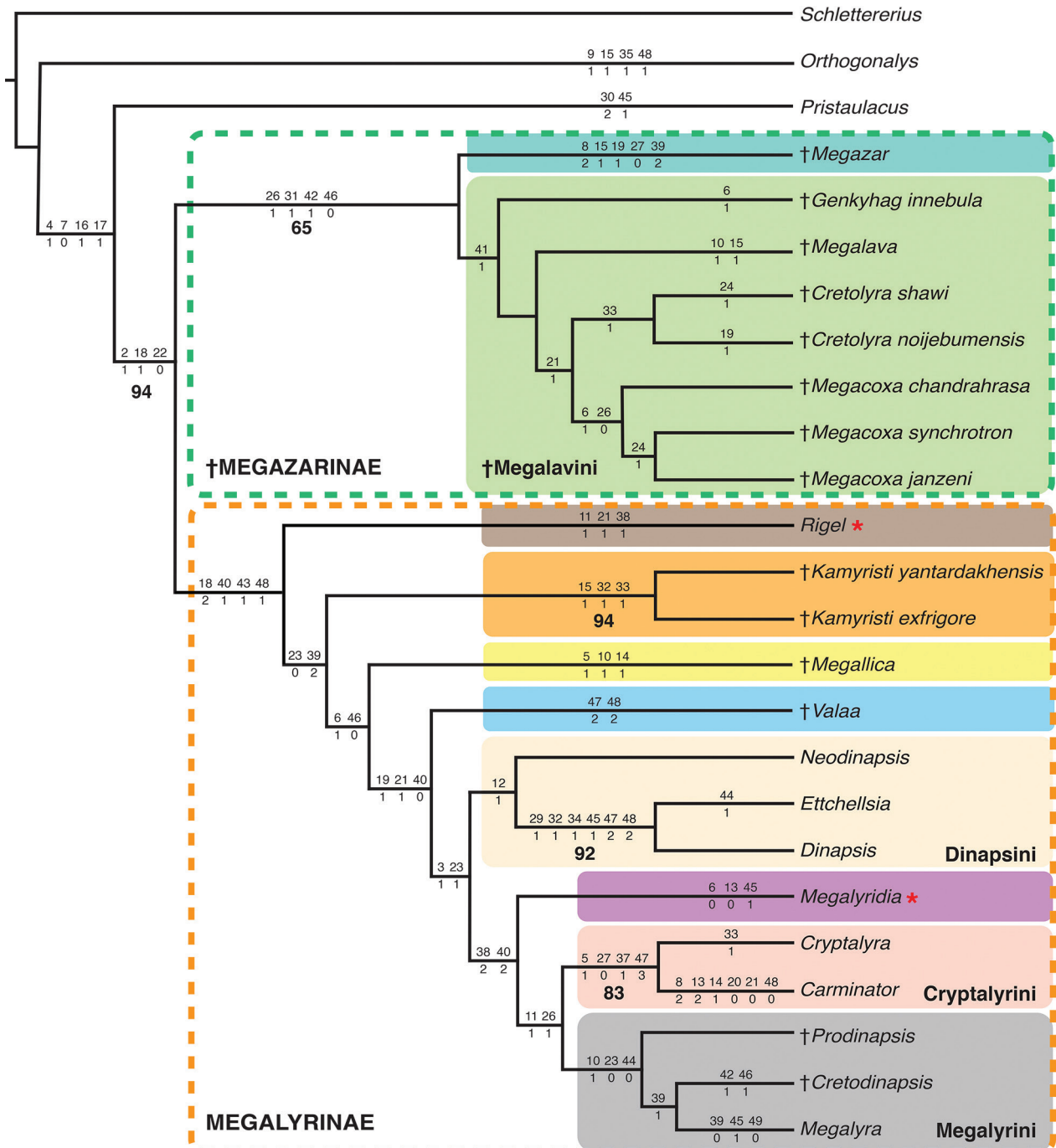


Figure 10. Cladogram of score 10.7779 retrieved by implied-weights analyses with $k = 5$. Unambiguous changes are indicated on the branches; bootstrap support values > 60 are shown in bold below nodes; red stars indicate placement of taxa conflicting with the results of the Bayesian analyses.

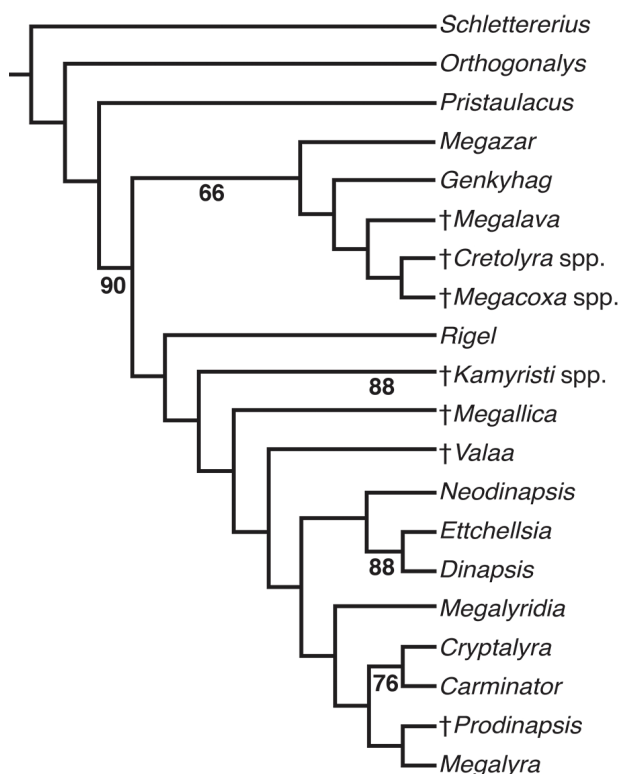


Figure 11. Cladogram of score 10.2560 retrieved by implied-weights analyses with $k = 5$ and \dagger *Cretodinapsis* excluded. Bootstrap support values > 60 are shown below nodes.

but not in the equal rates model (Mkv BPP < 0.50). On the contrary, *Megalyra* + \dagger *Cretodinapsis* + \dagger *Prodinapsis* + *Carminator* + *Cryptalyra* is supported under the equal rates model (Mkv BPP ~ 0.64) whereas the variable rates model does not support it (Mkv+G BPP < 0.50). The only consistent conflict between Bayesian and parsimony is the recovery of *Rigel* as sister to *Megalyridia* rather than to the remaining Megalyrinae under the equal rates model (Mkv BPP ~ 0.56); character state transitions that support this and other possible clades are reported in Table 2.

5. Discussion

The analyses of Vilhelmsen et al. (2010a) did not clearly demonstrate synapomorphies and retrieve the monophyly of all tribes, after the large expansion of the fossil record by Perrichot (2009). By adding four new tribes, four new genera and eight new species in the present study, we hope to clarify character evolution and resolve the relationships between the genera of Megalyridae. Interestingly, the topology retrieved here (Fig. 10) resembles figures 6C and 7 of Vilhelmsen et al. (2010a), more than their preferred topology (Vilhelmsen et al. 2010a: fig. 8). The results of the Bayesian analyses are also congruent with the trees presented here in figures 10 and 11 with the sole exception of a consistent sister group relationship between *Rigel* and *Megalyridia*. We retrieve the two subfam-

ilies \dagger Megazarinae **stat. nov.** and Megalyrinae as sister groups, albeit moderately supported. The entirely extinct \dagger Megazarinae **stat. nov.** are supported by the presence of a sinuate posterior mesopleural margin (26:1), comb-like spines along the inner margin of the hind leg (31:1; may be absent in the male of \dagger *M. truncata*) and the medial cell located posteriorly, at most half the width of the submarginal cell (42:1). Although not strongly supported in Bayesian analyses (BPP < 0.50), the \dagger Megalavini **trib. nov.** are retrieved as a clade in the maximum parsimony analyses. The main synapomorphy for this group is the position of the vein Rs+M, aligned with the M+Cu (41:1), rather than anterior to it. This, combined with the characters that have been discussed earlier, allows us to define \dagger *Megazar* as distinct from \dagger Megalavini **trib. nov.** The remaining megalyrids are united in Megalyrinae, a crown group clade composed of extant and extinct genera, corroborated by the anterior thoracic spiracle being fully surrounded by cuticle (18:2), the Rs vein reduced between Rs+M and r-rs (40:1), the M+Cu vein being colourless (43:1, pigmented in \dagger *Cretodinapsis*) and the propodeum areolate-rugose (48:1). \dagger *Kamyristi* **gen. nov.** is supported by the strong arch of the occipital carina (15:1), the erect metatibial setae (32:1), shared with [*Etchellsia* + *Dinapsis*], and the presence of one metatibial spur (33:1). Even though \dagger *Kamyristi* **gen. nov.** displays some similarities to members of the Dinapsini *sensu* Perrichot (2009), the inclusion of the new genus and the other fossil genera \dagger *Megallica* and \dagger *Valaa* renders the tribe paraphyletic. It is therefore better to exclude \dagger *Kamyristi* **gen. nov.**, \dagger *Megallica*, and \dagger *Valaa* from the Dinapsini and to propose three new monotypic tribes, one for each genus, namely \dagger Kamyristini **trib. nov.**, \dagger Megallicini **trib. nov.**, and \dagger Valaaini **trib. nov.** The monophyly of extant Dinapsini (i.e., *Dinapsis*, *Etchellsia*, *Neodinapsis*) is retrieved in the parsimony analyses, supported by the presence of a postocular carina (12:1; also present in some \dagger *Prodinapsis*). *Neodinapsis* is the sister group of [*Etchellsia* + *Dinapsis*], the latter congruently supported in the Bayesian analyses, and corroborated by the longitudinal carina on metacoxa (29:1), the erect metatibial setae (32:1), the shorter metatarsomeres 2–4 (34:1), the infumate banding patterns (45:1), the hind wing Rs short (47:2) and the carinate propodeum (48:2). The monophyly of Cryptalyrini (= *Carminator* + *Cryptalyra*) is once again retrieved, supported by the same characters as previously (Vilhelmsen et al. 2010a) and corroborated in all analyses.

Finally, we retrieve a clade composed of \dagger Cretodinapsini and Megalyrini, with \dagger *Prodinapsis* sister to [\dagger *Cretodinapsis* + *Megalyra*] under parsimony. The clade uniting these three genera is supported by the presence of a median sulcus on the vertex (10:1), the absence of parapsides (23:0) and the absence of 1A distally of cu-a (44:0). In addition, they form a polytomy with Cryptalyrini under the Mkv model. Under parsimony and Bayesian analyses, where the topology of this group is largely unresolved, the grouping of *Megalyra* + \dagger *Cretodinapsis* + \dagger *Prodinapsis* should be considered with caution given the relative homoplasy of these three characters and the numerous missing entries for \dagger *Cretodinapsis* (53%). Re-

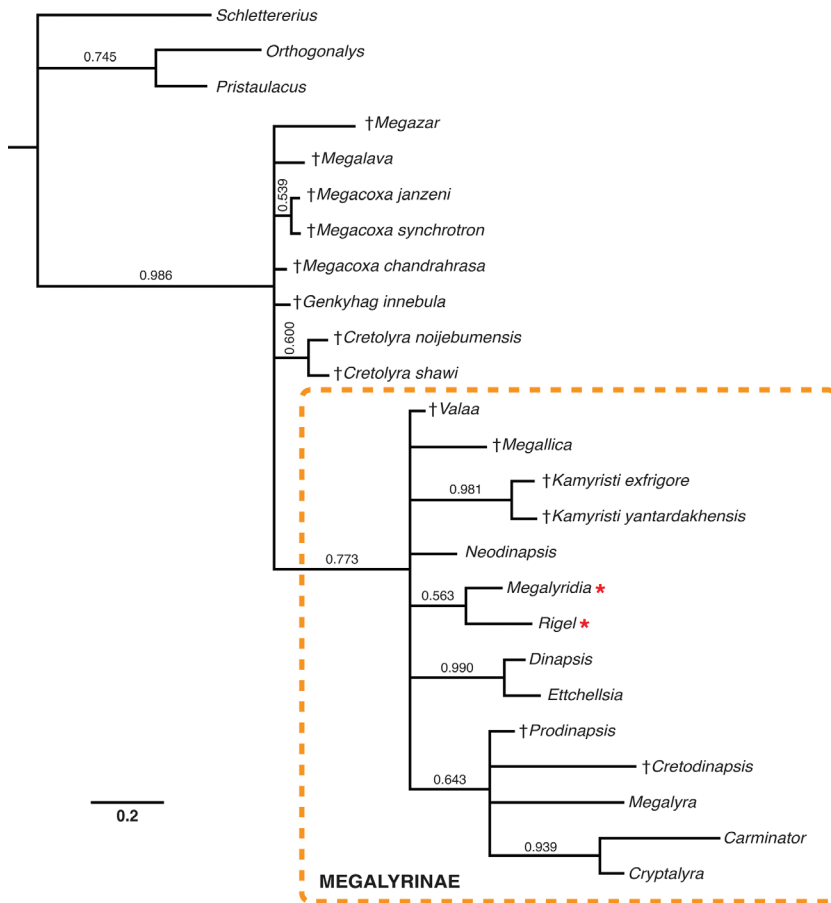


Figure 12. Phylogram retrieved by Bayesian analyses under equal rates model (Mkv) and a 0.5 Bayesian posterior probability cutoff. Bayesian posterior probabilities are indicated on the branches; red stars indicate placement of taxa conflicting with the results of the parsimony analyses; orange rectangle indicates the Megalyrinae subfamily as a monophyletic group.

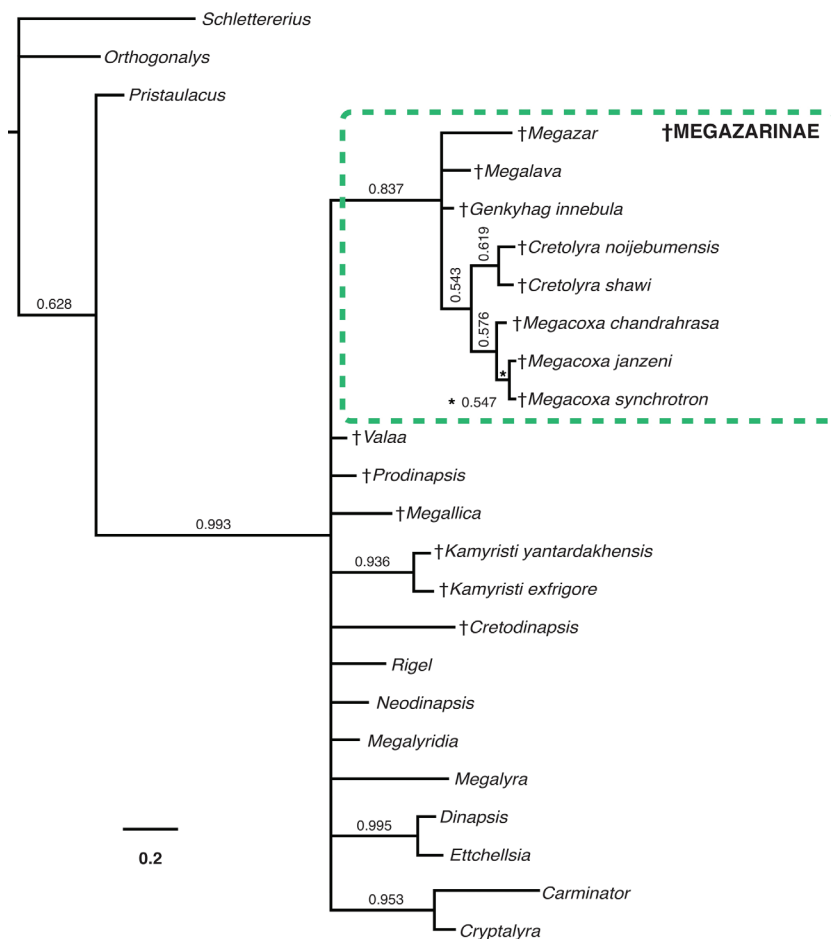


Figure 13. Phylogram retrieved by Bayesian analyses under variable rates model (Mkv+G) and a 0.5 Bayesian posterior probability cutoff. Bayesian posterior probabilities are indicated on the branches; green rectangle indicates the †Megazarinae subfamily as a monophyletic group.

Table 2. Ancestral state transitions estimated in MrBayes under the Mkv model. The degree of support for estimated synapomorphies is indicated via asterisks (*), three asterisks being the highest degree of support. “State fixed” indicates high support for daughter node coupled with uncertainty at the parent node due to state heterogeneity in other members of the clade. “*Megalyra–Carminator* clade” = †*Cretodinapsis* + *Megalyra* + †*Prodinapsis* + (*Carminator* + *Cryptalyra*).

Char	State	BPP	State	BPP	Interpretation
(A)	Megalyridae node		Megazarinae node		—
31	0	0.64	1	0.96	State fixed at daughter node
42	0	0.62	1	0.98	State fixed at daughter node
(B)	Megalyridae node		Megalyrinae node		—
18	1	0.51	2	0.96	State fixed at daughter node
39	1	0.77	2	0.97	State fixed at daughter node
43	0	0.78	1	0.97	State fixed at daughter node
44	0	0.79	1	0.91	State fixed at daughter node
(C)	Megalyrinae node		<i>Rigel</i> + <i>Megalyridia</i> node		—
6	1	0.84	0	0.99	State fixed at daughter node
13**	1	1.00	0	0.95	Well-supported synapomorphy
23	0	0.54	1	0.99	State fixed at daughter node
24	1	0.68	0	0.99	State fixed at daughter node
30**	0	0.93	1	1.00	Well-supported synapomorphy
47	2	0.75	1	1.00	State fixed at daughter node
48	2	0.81	1	1.00	State fixed at daughter node
49	2	0.78	1	0.97	State fixed at daughter node
(D)	Megalyrinae node		<i>Megalyra–Carminator</i> node		—
10**	0	0.97	1	0.85	Well-supported synapomorphy (note 1)
11**	0	0.99	1	0.93	Well-supported synapomorphy
30*	0	0.93	2	0.62	Weakly supported synapomorphy
38***	0	1.00	2	0.98	Highly supported synapomorphy (note 2)
40**	0	0.96	2	0.77	Well-supported synapomorphy (note 3)
44**	1	0.91	0	0.87	Well-supported synapomorphy (note 4)
(47*)	2	0.75	1	0.97	Very weakly supported synapomorphy (note 5)
48**	2	0.81	1	1.00	Well-supported synapomorphy (note 6)

Note 1. Implies synapomorphic reversal to 0 for *Cryptalyra* + *Carminator*.
Note 2. Variable in *Megalyra*; derivation of state 2 in *Megalyridia* implied to be homoplastic.
Note 3. Variable in †*Prodinapsis*; derivation of state 2 in *Megalyridia* implied to be homoplastic.
Note 4. Derivation of state 1 for *Cryptalyra* + *Carminator* implied to be synapomorphic.
Note 5. Pattern driven by †*Prodinapsis*; highly variable across tree; should be treated with skepticism.
Note 6. Implies derivation of state 1 for *Rigel* + *Megalyridia* is a homoplastic synapomorphy.

garding †*Cretodinapsis*, when this taxon is excluded from the parsimony analyses, †*Prodinapsis* is still retrieved as sister of *Megalyra* (Fig. 11), supported by the absence of parapsides (23:0) and the absence of 1A distally of cu-a (44:0). This sistergroup relationship is furthermore corroborated by the paleodistribution of the two genera, *Megalyra* being represented in Baltic amber, where †*Prodinapsis* is also widely found (Poinar and Shaw 2007; Perrichot 2009). On the other hand, under the conditions of the Bayesian analyses, the clade of †*Prodinapsis*, †*Cretodinapsis*, *Megalyra*, and *Cryptalyrini* is supported by seven characters (Table 2): presence of the median sulcus on the vertex and eye setae (10:1, 11:1), rugose metacoxal sculpture (30:2), absence of the fore wing Rs (38:2, 40:2), fore wing distal 1a darkened (44:0), and areolate-rugose propodeal sculpture (48:1). Therefore, the †*Cretodinapsini* is synonymized with *Megalyrini*, which is now composed of three genera.

Under Bayesian analyses, we also found support for the clade [*Rigel* + *Megalyridia*], which conflicts with the results of the parsimony analyses. With the equal rates

model, this grouping considerably strengthens the relationship of [*Megalyra* + †*Cretodinapsis* + †*Prodinapsis* + (*Carminator* + *Cryptalyra*)] (Fig. 12). [*Rigel* + *Megalyridia*] is supported by the flagellum longer than head + mesosoma (6:0, also in †*Cretolyra* **gen. nov.**, †*Kamyristi* **gen. nov.**, †*Megalava*, *Ettchellsia*, and the outgroup), the occipital carina basally curving towards the back the of head (13:0), the parapsides present (23:1, also in most Cretaceous taxa and all extant genera except *Megalyra*), the axillae continuous medially (24:0, also in *Dinapsis*, *Carminator*, *Ettchellsia*, *Megalyra*, *Neodinapsis* and some Cretaceous taxa), the metacoxa shagreened (30:1, also in *Carminator*, *Dinapsis*, *Neodinapsis* and †*Kamyristi exfrigore* **gen. et sp. nov.**), the Rs vein of the hind wing medium-sized (47:1, also in *Neodinapsis* and †*Prodinapsis*), the propodeum areolate-rugose (48:1, also in *Cryptalyra*, *Megalyra*, *Neodinapsis*, †*Cretodinapsis*, †*Kamyristi* **gen. nov.**, †*Megallica* and †*Prodinapsis*) and the ovipositor about as long as the body (49:1, also in *Dinapsis*, †*Megazar* and †*Prodinapsis*). Most of these characters are very homoplastic, except for the configuration

of the occipital carina, which is unique within the family. This finding highlights the instability of the relationships within the Megalyrinae, mainly because of the wide morphological diversity between and even within genera and the incomplete coding of some fossils.

The addition of new fossil taxa to the Megalyridae is not without consequences for the classification of the family. Only two of the non-monotypic tribes previously defined are consistently retrieved and can be diagnosed precisely (†Megalavini **trib. nov.**, Cryptalyrini); two others, Dinapsini *s.l.* and †Cretodinapsini, are not retrieved as monophyletic. To properly align classification with phylogeny, following the current tribal system, we propose a number of changes in the Megalyridae classification. First, we recognize the two main megalyrinid clades as subfamilies, the †Megazarinae **stat. nov.** and Megalyrinae. These two subfamilies are likely to represent distinct lineages within the Megalyridae, the †Megazarinae **stat. nov.** comprising exclusively Cretaceous taxa and the Megalyrinae constituting the crown group including all the extant taxa as well as a mix of extinct taxa from the Cretaceous onwards. Secondly, under parsimony, four additional non-conflicting groupings above the genus level are retrieved and can be consistently diagnosed and recognized as tribes: Cryptalyrini, Dinapsini *s.str.*, Megalyrini (expanded with the inclusion of †Cretodinapsini), and †Megalavini **trib. nov.** Finally, three new monotypic tribes are created for Cretaceous genera, †Kamyristini **trib. nov.**, †Megallicini **trib. nov.**, and †Valaaini **trib. nov.** Such a large number of tribes (ten, of which six are monotypic) may seem exaggerated for a group as relictual as the Megalyridae but is necessary to maintain congruence with the phylogenetic results. Furthermore, the Megalyridae are an ancient family, whose past diversity is only at the dawn of its discovery and those tribes could prove of use for future taxonomic works. A summary of the revised classification is presented in Appendix S1.

Vilhelmsen et al. (2010a) stated that †*Cretodinapsis* should be considered as an incertae sedis member of Evaniomorpha despite the presence of several characters reminiscent of the Megalyridae; these characters are probably plesiomorphic and not unique to the family (e.g., the vertex with a sulcus, the mesoscutum with a median mesoscutal sulcus, the large axillae, the similar fore wing venation, the long ovipositor). However, it has so far not been possible to establish the presence of a sub-antennal groove and the configuration of the anterior thoracic spiracle in †*Cretodinapsis*. While †*Cretodinapsis* usually jumped around depending on the parameters in the analyses of Vilhelmsen et al. (2010a), they retrieved it nested with extant genera when the †Maimetshidae were excluded. Its position within the Megalyrinae is more stable in our analyses but still poorly supported. This would strengthen the placement of †*Cretodinapsis* among the Megalyridae. However, it is unique in the subfamily in having the vein M+Cu pigmented on the forewing while it is spectral to absent in other megalyrines. This resembles more the †Megazarinae **stat. nov.**, but the venation is much reduced compared to other species and without

clarifying the diagnostic characters, it is not possible to decide further on the position of †*Cretodinapsis*. However, the material is unavailable for study at this time.

Hopefully, further improvement of the understanding of the phylogeny of Megalyridae will be achieved through the study of the fossil record. However, we do not currently know of megalyrinid morphotypes in Burmese amber in addition to those we describe here; Perrichot (2009) widely surveyed fossils from European Cretaceous and Paleogene ambers. New data could be provided by the descriptions of taxa in geographically distinct deposits such as the Aptian Congolese amber, Turonian Raritan amber, Campanian Canadian amber, lower Eocene Fushun (China) and Cambay (India) amber, and lower–middle Miocene Ethiopian and Zhangpu (China) amber.

6. Conclusions

The description of new fossil Megalyridae has enhanced our understanding of the evolutionary history of this family. It is evident that the Megalyridae experienced extensive radiation by the mid-Cretaceous, apparently including possible close relatives of at least some of the extant genera; however, a substantial portion of the Cretaceous diversity, i.e., the †Megazarinae **stat. nov.**, did not leave any extant descendants. The general decline in diversity and contraction of distribution of the family, correlated with environmental changes (i.e., a general cooling during the Cenozoic), is highlighted by the documentation of species from Siberia, located higher than 65° N during Upper Cretaceous (Rasnitsyn et al. 2016; Nadein and Perkovsky 2018), and now under a polar climate. Whereas fossil megalyrinids were only known from regions where they are presently absent, the Burmese amber taxa that are described herein are the first fossils found in a paratropical habitat in which they are currently present (i.e., *Ettchellsia* and *Carminator*). Thus, during the warm climate of the mid-Cretaceous, the Megalyridae appear to be at least as—and likely more—diverse compared to the present, the Cretaceous genera surpassing the modern genera in number, and possibly more widely distributed, although confirmed megalyrinid fossils from Gondwana deposits are still missing.

7. Author contributions

Manuel Brazidec: Conceptualization; data curation; formal analysis; investigation; methodology; project administration; writing – original draft; writing – review and editing; visualization; validation. **Lars Vilhelmsen:** Conceptualization; formal analysis; investigation; methodology; resources; writing – review and editing; validation. **Brendon E. Boudinot:** Formal analysis; funding acquisition; investigation; methodology; resources; writing – review and editing; visualization; validation. **Adrian K. F. Richter:** Methodology; resources; writing – review and editing; visualization; validation. **Jörg U. Hammel:** Methodology; resources; writing – review and editing; visualization; validation. **Evgeny**

E. Perkovsky: Funding acquisition; resources; writing – review and editing; validation. **Yong Fan:** Resources; writing – review and editing; validation. **Zhen Wang:** Resources; writing – review and editing; visualization; validation. **Qiong Wu :** Resources; writing – review and editing; visualization; validation. **Bo Wang:** Funding acquisition; resources; writing – review and editing; visualization; validation. **Vincent Perrichot:** Conceptualization; data curation; funding acquisition; investigation; methodology; project administration; resources; writing – review and editing; visualization; supervision; validation.

8. Competing interests

The authors have declared that no competing interests exist.

9. Acknowledgments

We are very grateful to all persons and colleagues who kindly provided or facilitated access to the material studied here: the late Jens-Wilhelm Janzen and his daughter Eva (Seevetal, Germany); and Prof. Alexandr Rasnitsyn (PIN, Russia). We warmly thank the editorial team of Arthropod Systematics & Phylogeny and two anonymous reviewers for careful consideration and suggestions on our manuscript. We thank the Willi Hennig Society for making available the TNT software for free. This research was supported by the National Natural Science Foundation of China (42125201) and Second Tibetan Plateau Scientific Expedition and Research (2019QZKK0706). This work is a contribution to the Deep-time Digital Earth (DDE) Big Science Program. B.E.B. was supported by an Alexander von Humboldt research fellowship (2020–2022) and a Peter S. Buck research fellowship from the Smithsonian Institution (2023). We acknowledge provision of beamtime, related to the proposal BAG-20190010 and I-20200136- at beamline P05 at PETRA III at DESY, a member of the Helmholtz Association (HGF), and the support during the beam times by Hereon team members Fabian Wilde, Julian Moosmann, and Felix Beckmann. This research was supported in part through the Maxwell computational resources operated at Deutsches Elektronen-Synchrotron DESY, Hamburg, Germany. E.E.P. acknowledge the support of Scholars at Risk Ukraine (SARU) jointly funded by the Villum Foundation, Carlsberg Foundation and Novo Nordisk Foundation.

10. References

- Baltazar CR (1962) *Ettchellsia philippinensis* sp. nov. (Dinapsinae, Megalyridae, Hymenoptera). The Philippine Journal of Science 90: 219–220.
- Blaimer BB, Santos BF, Cruaud A, Gates MW, Kula RR, Miko I, Rasplus J, Smith DR, Talamas EJ, Brady SG, Buffington, ML (2023) Key innovations and the diversification of Hymenoptera. Nature Communications 14(1): 1212. <https://doi.org/10.1038/s41467-023-36868-4>
- Castro LR, Dowton M (2006) Molecular analyses of the Apocrita (Insecta: Hymenoptera) suggest that the Chalcidoidea are sister to the diaprioid complex. Invertebrate Systematics 20(5): 603–614. <https://doi.org/10.1071/IS06002>
- Chen H, Liuhe B, Zhang X (2021) Two new species of the family Megalyridae (Hymenoptera) from China. ZooKeys 1043: 21–31. <https://doi.org/10.3897/zookeys.1043.65223>
- Cruikshank RD, Ko K (2003) Geology of an amber locality in the Hukawng Valley, Northern Myanmar. Journal of Asian Earth Sciences 21(5): 441–455. [https://doi.org/10.1016/S1367-9120\(02\)00044-5](https://doi.org/10.1016/S1367-9120(02)00044-5)
- Dowton M, Austin AD (2001) Simultaneous analysis of 16S, 28S, COI and morphology in the Hymenoptera: Apocrita – evolutionary transitions among parasitic wasps. Biological Journal of the Linnean Society 74(1): 87–111. <https://doi.org/10.1006/bjll.2001.0577>
- Dowton M, Austin AD, Dillon N, Bartowsky E (1997) Molecular phylogeny of the apocritan wasps: the Proctotrupomorpha and Evaniomorpha. Systematic Entomology 22(3): 245–255. <https://doi.org/10.1046/j.1365-3113.1997.d01-42.x>
- Engel MS (2016) A new genus and species of maimetshid wasps in Lebanese Early Cretaceous amber (Hymenoptera: Maimetshidae). Novitates Paleontologicae 18: 1–14. <https://doi.org/10.17161/np.v0i18.6497>
- Engelkes K, Friedrich F, Hammel JU, Haas A (2018) A simple setup for episcopic microtomy and a digital image processing workflow to acquire high-quality volume data and 3D surface models of small vertebrates. Zoomorphology 137(1): 213–228.
- Gibson GAP (1985) Some pro- and mesothoracic structures important for phylogenetic analysis of Hymenoptera, with reviews of terms used for the structures. Canadian Entomologist 117(11): 1395–1443. <https://doi.org/10.4039/Ent1171395-11>
- Goloboff PA, Catalano, SA (2016) TNT version 1.5, including a full implementation of phylogenetic morphometrics. Cladistics 32(3): 221–238. <https://doi.org/10.1111/cla.12160>
- Greving I, Wilde F, Ogurreck M, Herzen J, Hammel JU, Hipp A, Friedrich F, Lottermoser L, Dose T, Burmester H, Müller M, Beckmann F (2014) P05 imaging beamline at PETRA III: first results. In: Stuart RS (Ed) Proceedings of SPIE - Developments in X-Ray Tomography IX, Vol. 9212. San Diego, 921200-8.
- Grimaldi DA, Engel, MS (2005) Evolution of the insects. Cambridge University Press, Cambridge, 755 pp.
- Grimaldi DA, Ross AJ (2017) Extraordinary Lagerstätten in amber, with particular reference to the Cretaceous of Burma. In: Fraser NC, Sues HD (Eds) Terrestrial Conservation Lagerstätten: Windows into the Evolution of Life on Land. Dunedin Press, Edinburgh, 287–342.
- Grimaldi DA, Engel MS, Nascimbene PC (2002) Fossiliferous Cretaceous amber from Myanmar (Burma): Its rediscovery, biotic diversity, and paleontological significance. American Museum Novitates 3361: 1–71. [https://doi.org/10.1206/0003-0082\(2002\)361%3C0001:FCAFMB%3E2.0.CO;2](https://doi.org/10.1206/0003-0082(2002)361%3C0001:FCAFMB%3E2.0.CO;2)
- Grimaldi DA, Shadrinsky AM, Wampler TP (2000) A remarkable deposit of fossiliferous amber from the Upper Cretaceous (Turonian) of New Jersey. In: Grimaldi DA (Ed) Studies on Fossil in Amber with particular reference to the Cretaceous of New Jersey. Backhuys Publishers, Leiden, 1–76.
- Gumovsky A, Perkovsky EE, Rasnitsyn AP (2018) Laurasian ancestors and “Gondwanan” descendants of Rotoitidae (Hymenoptera: Chalcidoidea): What a review of Late Cretaceous *Baeomorpha* revealed. Cretaceous Research 84: 286–322. <https://doi.org/10.1016/j.cretres.2017.10.027>
- Haibel A, Ogurreck M, Beckmann F, Dose T, Wilde F, Herzen J, Müller M, Schreyer A, Nazmov V, Simon M, Last A, Mohr J (2010) Micro-and nano-tomography at the GKSS Imaging Beamline at PETRA III. Proceedings of SPIE – Developments in X-Ray Tomography VII 78040B. <https://doi.org/10.1117/12.860852>
- Huber JT, Sharkey MJ (1993) Structure. In: Goulet H, Huber JT (Eds) Hymenoptera of the world: An identification guide to families. Research Branch Agriculture Canada, Ottawa, 13–59.

- Kawada R, Barbosa D, Azevedo CO (2014) *Cryptalyra* (Hymenoptera, Megalyridae) from Maranhão, Brazil: three new species discovered after a large collecting effort. *ZooKeys* 442: 85–104. <https://doi.org/10.3897/zookeys.442.8237>
- Klopfstein S, Vilhemsen L, Heraty JM, Sharkey M, Ronquist F (2013) The Hymenopteran Tree of Life: Evidence from protein-coding genes and objectively aligned ribosomal data. *PLoS One* 8(8): e69344. <https://doi.org/10.1371/journal.pone.0069344>
- Lewis PO (2001) A likelihood approach to estimating phylogeny from discrete morphological character data. *Systematic Biology* 50(6): 913–925.
- Li L, Shih C, Rasnitsyn AP, Ren D (2015) New fossil ephialtids elucidating the origin and transformation of the propodeal-metasomal articulation of Apocrita (Hymenoptera). *BMC Evolutionary Biology* 15(1): 317. <https://doi.org/10.1186/s12862-015-0317-1>
- Lösel PD, van de Kamp T, Jayme A, Ershov A, Faragó T, Pichler O, Jerome NT, Aadepe N, Bremer S, Chilingaryan SA, Heethoff M, Kopmann A, Odar, J, Schmelzle S, Zuber M, Wittbrodt J, Baumbach T, Heuveline V (2020) Introducing Biomedisa as an open-source online platform for biomedical image segmentation. *Nature Communications* 11: 5577. <https://doi.org/10.1038/s41467-020-19303-w>
- Mao M, Gibson T, Dowton M (2014) Higher-level phylogeny of the Hymenoptera inferred from mitochondrial genomes. *Molecular Phylogenetics and Evolution* 84: 34–43. <https://doi.org/10.1016/j.ympev.2014.12.009>
- Mesaglio T, Shaw SR (2022) Observations of oviposition behaviour in the long-tailed wasp *Megalyra fasciipennis* Westwood, 1832 (Hymenoptera: Megalyridae). *Austral Ecology* 47(4): 889–893. <https://doi.org/10.1111/aec.13163>
- Mita T, Konishi K (2011) Phylogeny and biogeography of *Carminator* (Hymenoptera: Megalyridae). *Systematic Entomology* 36(1): 104–114. <https://doi.org/10.1111/j.1365-3113.2010.00548.x>
- Mita T, Shaw SR (2012) A taxonomic study on the genus *Ettchellsia* Cameron, with descriptions of three new species (Hymenoptera, Megalyridae, Dinapsini). *ZooKeys* 254: 99–108. <https://doi.org/10.3897/zookeys.254.4182>
- Mita T, Shaw SR (2020) A taxonomic study of *Dinapsis* Waterston, 1922 from Madagascar (Hymenoptera: Megalyridae, Dinapsini): crested wasps of the *hirtipes* species-group. *Zootaxa* 4858(1): 71–84. <https://doi.org/10.11646/zootaxa.4858.1.4>
- Moosmann J, Ershov A, Weinhardt V, Baumbach T, Prasad MS, La-Bonne C, Xiao X, Kashed, J, Hofmann R (2014) Time-lapse X-ray phase-contrast microtomography for in vivo imaging and analysis of morphogenesis. *Nature Protocols* 9(2): 294–304. <https://doi.org/10.1038/nprot.2014.033>
- Nadein KS, Perkovsky EE (2018) A new tribe of Galerucinae leaf beetle (Insecta: Coleoptera: Chrysomelidae) from the Upper Cretaceous Taimyr amber. *Cretaceous Research* 84: 97–106. <https://doi.org/10.1016/j.cretres.2017.10.023>
- Naumann ID (1987) A new megalyrid (Hymenoptera: Megalyridae) parasitic on sphecoid wasp in Australia. *Journal of the Australian Entomological Society* 26(3): 215–222. <https://doi.org/10.1111/j.1440-6055.1987.tb00289.x>
- Noble NS (1933) The citrus gall wasp (*Eurytoma fellis* Girault). *The Agricultural Gazette of New South Wales* 44: 465–469.
- Noble NS (1936) The citrus gall wasp (*Eurytoma fellis* Girault). *New South Wales Department of Agriculture Science* 53: 1–41.
- Palenstijn WJ, Batenburg KJ, Sijbers J (2011) Performance improvements for iterative electron tomography reconstruction using graphics processing units (GPUs). *Journal of Structural Biology* 176(2): 250–253.
- Pérez-de la Fuente R, Perrichot V, Ortega-Blanco J, Delclòs X, Engel MS (2012) Description of the male of *Megalava truncata* Perrichot (Hymenoptera: Megalyridae) in Early Cretaceous amber from El Soplao (Spain). *Zootaxa* 3274(1): 29–37. <https://doi.org/10.11646/zootaxa.3274.1.3>
- Perkovsky EE, Vasilenko DV (2019) A summary of recent results in the study of Taimyr amber. *Paleontological Journal* 53(10): 984–993. <https://doi.org/10.1134/S0031030119100149>
- Perkovsky EE, Wegierek P (2017) Oldest amber species of Palaeoaphididae (Hemiptera) from Baikura (Taimyr amber). *Cretaceous Research* 80: 56–60. <https://doi.org/10.1016/j.cretres.2017.08.013>
- Perrichot V (2009) Long-tailed wasps (Hymenoptera: Megalyridae) from Cretaceous and Paleogene European amber. *Paleontological Contributions* 1: 1–19. <https://doi.org/10.17161/PC.1808.5468>
- Perrichot V, Nel A, Néraudeau D (2004) A new, enigmatic, evaniomorph in the Albian amber of France (Insecta, Hymenoptera). *Journal of Systematic Palaeontology* 2(2): 159–162. <https://doi.org/10.1017/S1477201904001245>
- Poinar GO, Shaw SR (2007) *Megalyra baltica* Poinar and Shaw n. sp. (Hymenoptera: Megalyridae), a long-tailed wasp from Baltic amber. *Zootaxa* 1478(1): 65–68. <https://doi.org/10.11646/zootaxa.1478.1.7>
- Rambaut A, Drummond AJ, Xie D, Baele G, Suchard MA (2018) Posterior summarisation in Bayesian phylogenetics using Tracer 1.7. *Systematic Biology* 67(5): 901–904. <https://doi.org/10.1093/sysbio/syy032>
- Rasnitsyn AP (1975) Hymenoptera Apocrita of Mesozoic. *Trudy Paleontologicheskogo Instituta Akademii Nauk SSSR* 147: 1–134 [In Russian].
- Rasnitsyn, AP (1977) New Hymenoptera from the Jurassic and Cretaceous of Asia. *Paleontologicheskii Zhurnal* 1977(3): 98–108 [In Russian, English translation in *Paleontological Journal* 1978(11): 349–357].
- Rasnitsyn AP (1988) An outline of evolution of the hymenopterous insects (Order Vespida). *Oriental Insects* 22(1): 115–145. <https://doi.org/10.1080/00305316.1988.11835485>
- Rasnitsyn AP (2002) Superorder Vespidea Laicharting, 1781. Order Hymenoptera Linné, 1758 (= Vespida Laicharting, 1781). In: Rasnitsyn AP, Quicke DLJ (Eds) *History of Insects*. Kluwer Academic Publishers, Dordrecht: 242–254.
- Rasnitsyn AP, Brothers DJ (2009) New genera and species of Maimetshidae (Hymenoptera: Stephanoidea s.l.) from the Turonian of Botswana, with comments on the status of the family. *African Invertebrates* 50(1): 191–204. <https://doi.org/10.5733/afin.050.0108>
- Rasnitsyn AP, Öhm-Kühnle C (2021) Non-acuteate Hymenoptera in the Cretaceous ambers of the world. *Cretaceous Research* 124: 104805. <https://doi.org/10.1016/j.cretres.2021.104805>
- Rasnitsyn AP, Zhang H (2010) The early evolution of Apocrita (Insecta, Hymenoptera) as indicated by new findings in the Middle Jurassic of Daohugou, Northeast China. *Acta Geologica Sinica (English Edition)* 84(4): 834–873. <https://doi.org/10.1111/j.1755-6724.2010.00254.x>
- Rasnitsyn AP, Bashkuev AS, Kopylov DS, Lukashovich ED, Ponomarenko AG, Popov YA, Rasnitsyn DA, Ryzhkova OV, Sidorchuk EA, Sukatsheva ID, Vorontsov DD (2016) Sequence and scale of changes in the terrestrial biota during the Cretaceous (based on materials from fossil resins). *Cretaceous Research* 61: 234–255. <http://dx.doi.org/10.1016/j.cretres.2015.12.025>

- Richter A, Boudinot BE, Yamamoto S, Katzke J, Beutel RG (2022) The first reconstruction of the head anatomy of a Cretaceous insect, †*Gerontofornica gracilis* (Hymenoptera: Formicidae), and the early evolution of ants. *Insect Systematics & Diversity* 6(5): 4. <https://doi.org/10.1093/isd/ixac013>
- Rodd NW (1951) Some observations on the biology of Stephanidae and Megalyridae (Hymenoptera). *Australian Zoologist* 11: 341–346.
- Ronquist F, Rasnitsyn AP, Roy A, Eriksson K, Lindgren M (1999) Phylogeny of the Hymenoptera: A cladistic reanalysis of Rasnitsyn's (1988) data. *Zoologica Scripta* 28: 13–50. <https://doi.org/10.1046/j.1463-6409.1999.00023.x>
- Ronquist F, Telsenko M, van der Mark P, Ayres DL, Darling A, Höhna S, Larget B, Liu L, Suchard MA, Huelsenbeck JP (2012) MRBAYES 3.2: Efficient Bayesian phylogenetic inference and model selection across a large model space. *Systematic Biology* 61(3): 539–542. <https://doi.org/10.1093/sysbio/sys029>
- Schindelin J, Arganda-Carreras I, Frise E, Kaynig V, Longair M, Pietzsch T, Preibisch S, Rueden C, Saalfeld S, Schmid B, Tinevez J, White DJ, Hartenstein V, Eliceiri K, Tomancak P, Cardona A (2012) Fiji: an open-source platform for biological-image analysis. *Nature Methods* 9(7): 676–682. <https://doi.org/10.1038/nmeth.2019>
- Schletterer A (1889) Die Hymenopteren-Gattungen *Stenophasmus* Smith, *Monomachus* Westwood, *Pelecinus* Latreille und *Megalyra* Westwood. *Berliner Entomologische Zeitschrift* 33: 197–250.
- Sharkey MJ (2007) Phylogeny and classification of Hymenoptera. *Zootaxa* 1668: 521–548. <https://doi.org/10.11646/zootaxa.1668.1.25>
- Sharkey MJ, Carpenter JM, Vilhelmsen L, Heraty J, Liljeblad J, Dowling APG, Schulmeister S, Murray D, Deans AR, Ronquist F, Krogmann L, Wheeler WC (2012) Phylogenetic relationships among superfamilies of Hymenoptera. *Cladistics* 28(1): 80–112. <https://doi.org/10.1111/j.1096-0031.2011.00366.x>
- Shaw SR (1987) Three new megalyrids from South America (Hymenoptera: Megalyridae). *Psyche* 94: 189–199. <https://doi.org/10.1111-55/1987/28207>
- Shaw SR (1988) *Carminator*, a new genus of Megalyridae (Hymenoptera) from the Oriental and Australian regions, with a commentary on the definition of the family. *Systematic Entomology* 13: 101–113. <https://doi.org/10.1111/j.1365-3113.1988.tb00233.x>
- Shaw SR (1990a) Phylogeny and biogeography of the parasitoid wasp family Megalyridae (Hymenoptera). *Journal of Biogeography* 17: 569–581. <https://doi.org/10.2307/2845141>
- Shaw SR (1990b) A taxonomic revision of the long-tailed wasps of the genus *Megalyra* Westwood (Hymenoptera: Megalyridae). *Invertebrate Taxonomy* 3: 1005–1052. <https://doi.org/10.1071/IT9891005>
- Shaw SR, van Noort S (2009) A new *Dinapsis* species from the Central African Republic (Hymenoptera, Megalyridae, Dinapsini). *Zootaxa* 2118(1): 30–36. <https://doi.org/10.11646/zootaxa.2118.1.2>
- Shi G, Grimaldi DA, Harlow GE, Wang Ji, Wang, Ju, Yang M, Lei W, Li Q, Li X (2012) Age constraint on Burmese amber based on U-Pb dating of zircons. *Cretaceous Research* 37: 155–163. <https://doi.org/10.1016/j.cretres.2012.03.014>
- Smith RDA, Ross AJ (2018) Amber ground pholadid bivalve borings and inclusions in Burmese amber: implications for proximity of resin producing forests to brackish waters, and the age of the amber. *Earth and Environmental Science Transactions of the Royal Society of Edinburgh* 107(2–3): 239–247. <https://doi.org/10.1017/S1755691017000287>
- Tang P, Zhu J, Zheng B, Wei S, Sharkey MJ, Chen X, Vogler, A (2019) Mitochondrial phylogenomics of the Hymenoptera. *Molecular Phylogenetics and Evolution* 131: 8–18. <https://doi.org/10.1016/j.ympev.2018.10.040>
- van Aarle W, Palenstijn WJ, de Beenhouwer J, Altantzis T, Bals S, Batenburg KJ, Sijbers J (2015) The ASTRA toolbox: A platform for advanced algorithm development in electron tomography. *Ultramicroscopy* 157: 35–47. <https://doi.org/10.1016/j.ultramic.2015.05.002>
- van Aarle W, Palenstijn WJ, Cant J, Janssens E, Bleichrodt F, Dabralovski A, De Beenhouwer J, Batenburg KJ, Sijbers J (2016) Fast and flexible X-ray tomography using the ASTRA toolbox. *Optics Express* 24(22): 25129–25147. <https://doi.org/10.1364/OE.24.025129>
- van Noort S, Shaw SR (2009) *Megalyridia capensis* (Hymenoptera: Megalyridae: Megalyridiini), a relict species endemic to South Africa. *African Natural History* 5(1): 1–8.
- van Noort S, Shaw SR, Copeland RS (2022) Revision of the endemic African genus *Dinapsis* (Dinapsini, Megalyridae, Hymenoptera) with description of seven new species. *ZooKeys* 1112: 27–122. <https://doi.org/10.3897/zookeys.1112.82307>
- Vilhelmsen L (2003) Flexible ovipositor sheaths in parasitoid Hymenoptera (Insecta). *Arthropod Structure and Development* 32(2–3): 277–287. [https://doi.org/10.1016/S1467-8039\(03\)00045-8](https://doi.org/10.1016/S1467-8039(03)00045-8)
- Vilhelmsen L, Perrichot V, Shaw SR (2010a) Past and present diversity and distribution in the parasitic wasp family Megalyridae (Hymenoptera). *Systematic Entomology* 35(4): 658–677. <https://doi.org/10.1111/j.1365-3113.2010.00537.x>
- Vilhelmsen L, Mikó I, Krogmann L (2010b) Beyond the wasp-waist: Structural diversity and phylogenetic significance of the mesosoma in apocritan wasps (Insecta: Hymenoptera). *Zoological Journal of the Linnean Society* 159(1): 22–194. <https://doi.org/10.1111/j.1096-3642.2009.00576.x>
- Waterston J (1922) A new family of Hymenoptera from South Africa. *Annals and Magazine of Natural History* 10(9): 418–420. <https://doi.org/10.1080/00222932208632792>
- Westwood JO (1832) Class Insecta. Supplement on the Hymenoptera. In: Griffith E (Ed) *The animal kingdom arranged in conformity with its organization by the Baron Cuvier*. Whittaker, Treacher and Co., London, 389–576.
- Wilde F, Ogurreck M, Greving I, Hammel JU, Beckmann F, Hipp A, Lottermoser L, Khokhriakov I, Lytaev P, Dose T, Burmester H, Müller M, Schreyer A (2016) Micro-CT at the imaging beamline P05 at PETRA III. *AIP Conference Proceedings* 1741: 030035. <https://doi.org/10.1063/1.4952858>
- Xia F, Yang G, Zhang Q, Shi G, Wang B (2015) *Amber: Lives through time and space*. Science Press, Beijing, 197 pp.
- Xie W, Lewis PO, Fan Y, Kuo L, Chen M (2011) Improving marginal likelihood estimation for Bayesian phylogenetic model selection. *Systematic Biology* 60(2): 150–160.
- Yang Z (1993) Maximum likelihood estimation of phylogeny from DNA sequences when substitution rates differ over sites. *Molecular Biology and Evolution* 10(6): 1396–1401.
- Yu T, Kelly R, Mu L, Ross AJ, Kennedy J, Broly P, Xia F, Zhang H, Wang B, Dilcher D (2019) An ammonite trapped in Burmese amber. *Proceedings of the National Academy of Sciences of the USA* 116(23): 11345–11350. <https://doi.org/10.1073/pnas.1821292116>
- Zhang Q, Rasnitsyn AP, Wang B, Zhang H (2018) Hymenoptera (wasps, bees and ants) in mid-Cretaceous Burmese amber: A review of the fauna. *Proceedings of the Geologists' Association* 129(6): 736–747. <https://doi.org/10.1016/j.pgeola.2018.06.004>

Supplementary Material 1

Appendices S1, S2

Authors: Brazidec M, Vilhelmsen L, Boudinot BE, Richter AKF, Hammel JU, Perkovksy EE, Fan Y, Whang Z, Wu Q, Wang B, Perrichot V (2024)

Data type: .zip

Explanation notes: **Appendix S1.** Revised classification of the Megalyridae. — **Appendix S2.** List of characters used in the phylogenetic analyses.

Copyright notice: This dataset is made available under the Open Database License (<http://opendatacommons.org/licenses/odbl/1.0>). The Open Database License (ODbL) is a license agreement intended to allow users to freely share, modify, and use this Dataset while maintaining this same freedom for others, provided that the original source and author(s) are credited.

Link: <https://doi.org/asp.82.e111148.suppl1>